

AD-A039 896

MCDONNELL AIRCRAFT CO ST LOUIS MO  
FOVEAL LENS SIZE REDUCTION STUDY.(U)  
APR 76 R W FISHER, R D HELMICK, E LICIS

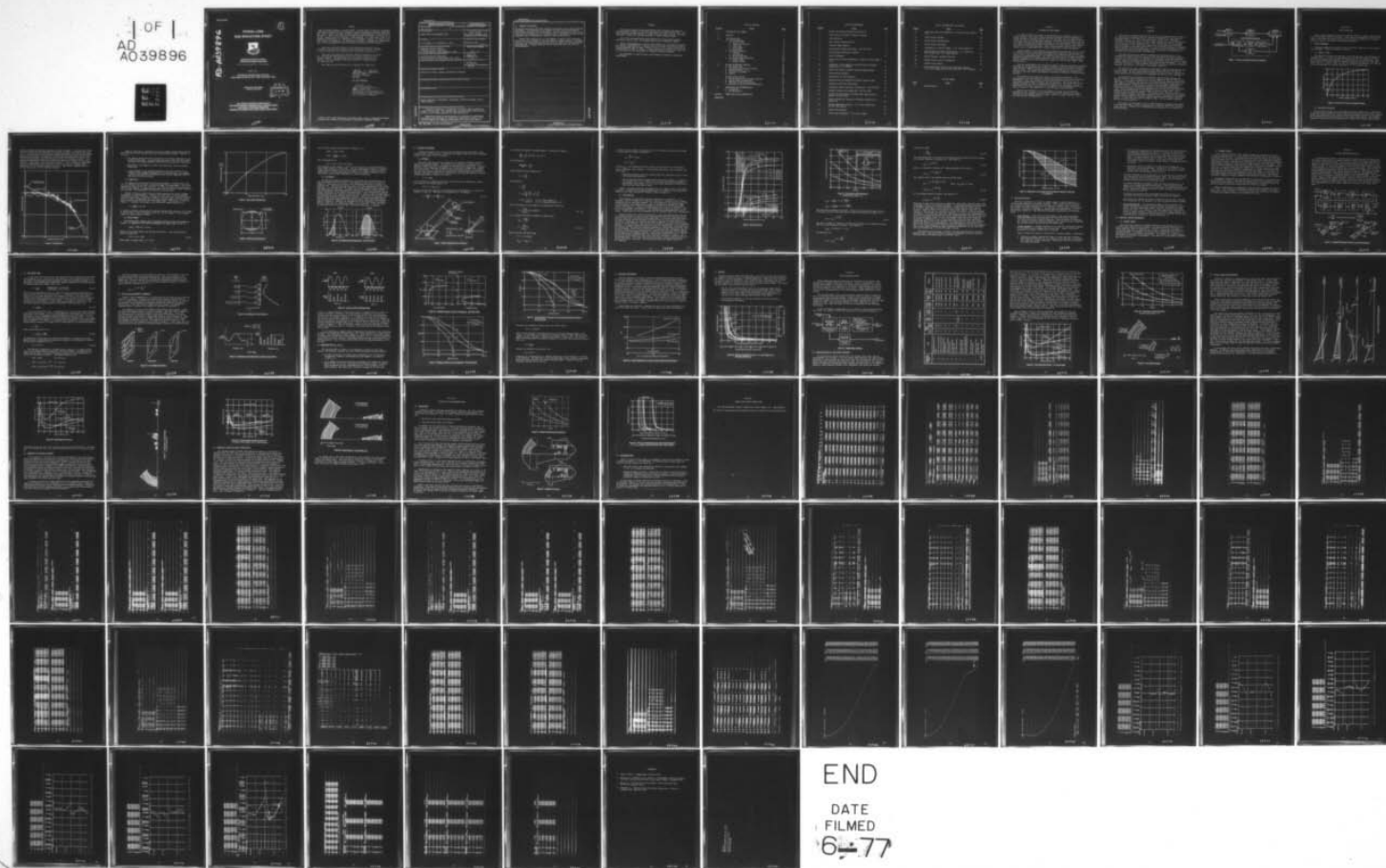
F/G 20/6

F33615-75-C-1294  
NL

UNCLASSIFIED

AFAL-TR-76-6

1 OF 1  
AD  
A039896



END

DATE  
FILMED  
6-77

AFAL-TR-76-6

AD-A039896

①  
B.S.

# FOVEAL LENS SIZE REDUCTION STUDY



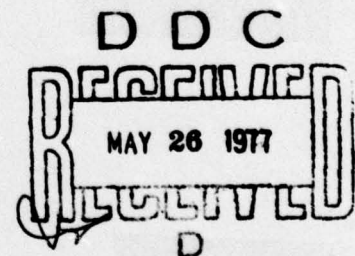
**McDonnell Aircraft Company  
McDonnell Douglas Corporation**

Box 516, Saint Louis, Missouri 63166 - Tel. (314)232-0232

April 1976

**TECHNICAL REPORT AFAL-TR-76-6  
Final Report for Period June 1975 - November 1975**

LEA  
Approved for public release;  
distribution unlimited.



**AIR FORCE AVIONICS LABORATORY  
AIR FORCE WRIGHT AERONAUTICAL LABORATORIES  
AIR FORCE SYSTEMS COMMAND  
WRIGHT-PATTERSON AIR FORCE BASE, OHIO 45433**

62728



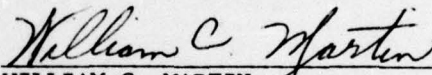
NOTICE

When Government drawings, specifications, or other data are used for any purpose other than in connection with a definitely related Government procurement operation, the United States Government thereby incurs no responsibility nor any obligation whatsoever; and the fact that the government may have formulated, furnished, or in any way supplied the said drawings, specifications, or other data, is not to be regarded by implication or otherwise as in any manner licensing the holder or any other person or corporation, or conveying any rights or permission to manufacture, use, or sell any patented invention that may in any way be related thereto.

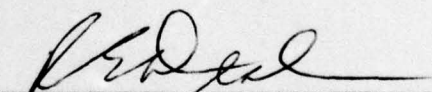
This report has been reviewed by the Information Office (OI) and is releasable to the National Technical Information Service (NTIS). At NTIS, it will be available to the general public, including foreign nations.

This report was prepared by McDonnell-Douglas Corporation, St. Louis, MO. The work was performed under Air Force Contract F33615-75-C-1294, Project 76620711. The program was under the technical direction of William C. Martin, AFAL/RWI, AF Avionics Laboratory, Wright-Patterson Air Force Base, OH.

This report has been reviewed and is approved for publication.

  
WILLIAM C. MARTIN  
AF Project Scientist  
AFAL/RWI

FOR THE COMMANDER

  
ROBERT E. DEAL, Chief  
Electro-Optics & Reconnaissance Br.  
Reconnaissance & Weapon Delivery Div.  
Air Force Avionics Laboratory

Copies of this report should not be returned unless return is required by security considerations, contractual obligations, or notice on a specific document.

62728

90

UNCLASSIFIED

SECURITY CLASSIFICATION OF THIS PAGE (When Data Entered)

REPORT DOCUMENTATION PAGE		READ INSTRUCTIONS BEFORE COMPLETING FORM
1. REPORT NUMBER AFAL-TR-76-6 ✓	2. GOVT ACCESSION NO.	3. RECIPIENT'S CATALOG NUMBER
4. TITLE (and Subtitle) FOVEAL LENS SIZE REDUCTION STUDY		5. TYPE OF REPORT & PERIOD COVERED Final Report June 1975 to November 1975
		6. PERFORMING ORG. REPORT NUMBER
7. AUTHOR(s) R. W. Fisher, R. D. Helmick, G. Licis		8. CONTRACT OR GRANT NUMBER(s) F33615-75-C-1294 <i>New</i>
9. PERFORMING ORGANIZATION NAME AND ADDRESS McDonnell Aircraft Company McDonnell Douglas Corporation P. O. Box 516, St. Louis, Missouri 63166		10. PROGRAM ELEMENT, PROJECT, TASK AREA & WORK UNIT NUMBERS 7662 07 11
11. CONTROLLING OFFICE NAME AND ADDRESS Air Force Avionics Laboratory Wright-Patterson Air Force Base, Ohio 45433		12. REPORT DATE April 1976
		13. NUMBER OF PAGES 90
14. MONITORING AGENCY NAME & ADDRESS (if different from Controlling Office)		15. SECURITY CLASS. (of this report) UNCLASSIFIED
		15a. DECLASSIFICATION/DOWNGRADING SCHEDULE
16. DISTRIBUTION STATEMENT (of this Report) Approved for public release; distribution unlimited.		
17. DISTRIBUTION STATEMENT (of the abstract entered in Block 20, if different from Report)		
18. SUPPLEMENTARY NOTES		
19. KEY WORDS (Continue on reverse side if necessary and identify by block number) Optical Detection, Intelligence, Subsystems, Television Systems, Optics, Remote Sensing		
20. ABSTRACT (Continue on reverse side if necessary and identify by block number) Technical feasibility is established of miniaturizing the MCAIR non-linear or foveal lens. The original lens fabricated under a Navy contract proved to be too large and heavy for USAF applications.  Theoretical limits of miniaturization are developed by establishing preliminary optical designs for lenses with progressively smaller clear aperture diameter and comparing performance with system requirements.		

62728

90



UNCLASSIFIED

SECURITY CLASSIFICATION OF THIS PAGE(When Data Entered)

20. ABSTRACT (Concluded).

The results show that a 50% size reduction is possible with no loss in optical performance. The resulting 4 inch diameter F/3 lens can be fabricated of either glass or plastic optical materials. Optical performance of the lens is such that it can support up to 4x magnification of its image to achieve a zoom capability that is desirable for detailed target identification.

Further size reduction to a 2 inch diameter is shown to be technically feasible but with a penalty of less resolution or higher F/number. The former will limit zoom magnification possible, while the latter will reduce daylight operating time. A higher technical risk is associated with this level of miniaturization.

UNCLASSIFIED

SECURITY CLASSIFICATION OF THIS PAGE(When Data Entered)

90

82728

80

## PREFACE

This report contains studies and analyses which establish the degree of miniaturization possible for the MCAIR non-linear or variable acuity lens. This lens, previously proven feasible in a large size under Navy contract, has great potential to reduce the required bandwidth of remote viewing systems.

This effort was administered under direction of the Air Force Avionic Laboratory, Dayton, Ohio. The program monitor was Mr. William C. Martin.

Special acknowledgement is made to Roger Helmick for the technical analysis and computer programming and to George Licis for his able technical assistance. Program management and the major technical portion of the written draft were the responsibility of Ralph W. Fisher. A major subcontractor during this effort was Mr. David Grey who was responsible for computer program development.

The assistance of these and many other McDonnell personnel is gratefully acknowledged.



# TABLE OF CONTENTS

<u>Section</u>	<u>Title</u>	<u>Page</u>
I	INTRODUCTION AND SUMMARY	1
II	APPROACH	2
III	INPUT DEFINITION	4
	A. Fixed Parameters	4
	1. Field of View	4
	2. Distortion Function	4
	3. Image Size	6
	4. Focal Length	6
	5. Wavelength	8
	B. Tradeoff Parameters	9
	1. F/Number	9
	2. Lens Quality	11
	3. Optical Materials	15
	C. Practical Design Constraints	16
	1. Element Shape	16
	2. Element Sizing	17
IV	SYSTEMS PERFORMANCE ANALYSIS	18
	A. The Sensor Lens	19
	B. The Optical/Electronic Conversion	20
	C. Remaining MTF's $\tau_3$ To $\tau_6$	22
	D. Observer Performance	25
	E. Results	26
V	OPTICAL DESIGN STUDIES	27
	A. Miniaturization in the Visual Spectrum	27
	B. Optical Relay Configuration	31
	C. Extension of Spectral Response	33
	D. Materials Study and Final Optimization	35
VI	CONCLUSIONS AND RECOMMENDATIONS	37
	A. Conclusions	37
	B. Recommendations	39
Appendix	SAMPLE LENS DESIGN COMPUTER RUN	40
REFERENCES		81

# LIST OF ILLUSTRATIONS

<u>Figure</u>	<u>Title</u>	<u>Page</u>
1	Foveal Lens Miniaturization Study Approach	3
2	Lens Size as a Function of Angular Coverage	4
3	Lens Distortion	5
4	Lens Transfer Characteristics	7
5	CCD/Lens Image Geometry	7
6	Lens Spectral Design Requirement - RCA SID 51232	8
7	Sensor/Target Photometric Geometry	9
8	Earth Illuminance	12
9	Theoretical Lens Size Parametrics - Effective Focal Length = 1 In.	13
10	Modulation at Lens Image for Critical Detector Response Frequencies ( $\alpha = 0.0305\text{mm}$ )	15
11	General RVS Optical Transfer Function Representation	18
12	Array Detector Geometry	20
13	Input/Output of Array Elements	21
14	Modulation and the Modulation Transfer Function (MTF)	21
15	Variation of MTF with Phase Angle	22
16	Probability Density Function of Modulation - RCA SID 51232	23
17	Maximum, Minimum, and Average MTF - RCA SID 51232	23
18	Theoretical MTF Compared to Conventional Representation Method - RCA SID 51232	24
19	Visual Threshold as Functions of Display Brightness and Resolution	25
20	Minimum Resolvable Contrast - 1 In. Focal Length Lens, RCA SID 51232 Sensor	26
21	Design Study Approach	27
22	Visual Lens Performance - 1 In. Focal Length	29

# LIST OF ILLUSTRATIONS (Concluded)

<u>Figure</u>	<u>Title</u>	<u>Page</u>
23	Theoretical Lens Size Parametrics - Effective Focal Length = 1 In.	30
24	Visual Optical Designs	30
25	Optical Relay Considerations	32
26	Optical Relay Performance	33
27	Configuration L Optical Design - 1 In. Focal Length F/3	34
28	Extended Spectral Range Configurations - 1 In. Effective Focal Length, F/3, 4 In. Clear Aperture	35
29	Optical Designs - Extended Spectrum	36
30	Revised Foveal Lens Size Parametrics	38
31	Possible Lens Layouts	38
32	Minimum Resolvable Contrast with Image Magnification - 1 In. Focal Length Lens Plus RCA SID 51232 - 100 fL Display	39

## LIST OF TABLES

<u>Table</u>	<u>Title</u>	<u>Page</u>
I	Run Description	28



## Section I

### INTRODUCTION AND SUMMARY

In 1969-1970 MCAIR conceived a unique technique for bandwidth reduction for remote viewing. This concept employs extreme non-linear optical components to divide the sensor's optical field of view into variable size resolution elements similar to that of the human visual process. When these picture elements are sent to a remote location and arranged (displayed) in the same geometry as received by the sensor, the resulting reconstructed picture will fully support human vision in both field of view and resolution. Total picture elements are such that transmission can be accomplished easily within conventional TV video bandwidths.

The key element of this Variable Acuity Remote Viewing System (the non-linear or "foveal" lens) was constructed and demonstrated during 1973 under contract to the U.S. Navy. This lens exceeded requirements for performance but was too large and heavy for USAF applications. The effort described in this document establishes technical feasibility of miniaturizing this lens and predicts its physical parameters, performance, and limitations when coupled to a solid state charge coupled sensing array.

This was accomplished by utilizing the computer design and optimization program, developed for our existing lens, to derive preliminary optical designs for smaller clear aperture diameters and the extended spectral range required for the silicon detector array. The theoretical performance of these designs are evaluated as a function of the performance requirements to determine the degree of miniaturization possible.

The results of this analytical effort far exceeded expectations. Size reductions over 50% are shown to be theoretically possible with no loss in optical performance. The 4 inch diameter F/3 lens resulting from this effort can be fabricated of either glass or plastic optical materials. Use of plastics for the aspheric elements can lead to significant production cost reductions. Optical performance of the lens is such that it can support up to 4x magnification of its image to achieve a zoom capability for detailed target identification.

Further size reduction to a 2 inch diameter is shown to be technically feasible but with a penalty of less resolution and higher F/number; the latter resulting in less daylight operating range. However, a higher technical risk is incurred with this configuration.



## Section II

### APPROACH

The Foveal Lens Miniaturization Study followed the sequence shown in Figure 1. Our existing lens parameters plus the customer recommended CCD characteristics furnished inputs to the "Input Definition" phase of the study. This phase, described in detail in Section 3 of this report, defined all information required to initiate the "optical design studies." This includes the fixed or constant inputs of field of view, distortion, image size, focal length, and wavelength. Also established in this phase are bounds for the tradeoff parameters of F/number, optical quality, and optical materials. In addition, practical design constraints are developed here such as minimum element size, mechanical considerations for materials, and fabrication/cost considerations.

The above data plus the computer optimization program developed for our existing lens supplied necessary inputs for the "Optical Design Study" discussed in Section 5 of this report. In parallel with this phase, a system performance analysis model was developed and exercised to continually assess the impact of lens quality outputs of the design studies on end-to-end system performance. This model, described in Section 4, outputs minimum resolvable contrast as functions of spatial frequency (resolution), lens quality, and display capability.

The heart of the study, the Optical Design Phase, begins by reducing the size of our existing lens while maintaining the same optical materials and optical spectral range. As this visual spectrum miniaturized lens evolved, a design study of the optical relay (identified as a requirement in Section 3) was conducted.

As confidence was developed in the modified computer design program, the optical spectral range is extended into one more compatible with the silicon CCD detector. At this point, materials are still maintained as glasses because of the wide range of dispersions and indices of refraction available in these materials. This simplifies the optimization by allowing continuous computer modeling of material constants. As the program converges on an optimized configuration, constraints are placed on materials characteristics so they match available glass types. After reoptimization of this design for specific glass types, it was evaluated over the effective response range of the silicon detector. Next, a plastic optical design was developed. To accomplish this, constraints were placed on the program to operate with plastic material optical constants for the aspheric elements (cost/performance tradeoffs indicate that spherical elements should be glass). At this point, two optical designs existed - one for plastic aspherics and one for glass aspherics.

In Section 6 of this report, the two final designs are assessed with respect to system performance, degree of miniaturization achieved, fabrication considerations, and cost. Finally, our recommendations are presented for an approach to lens development.

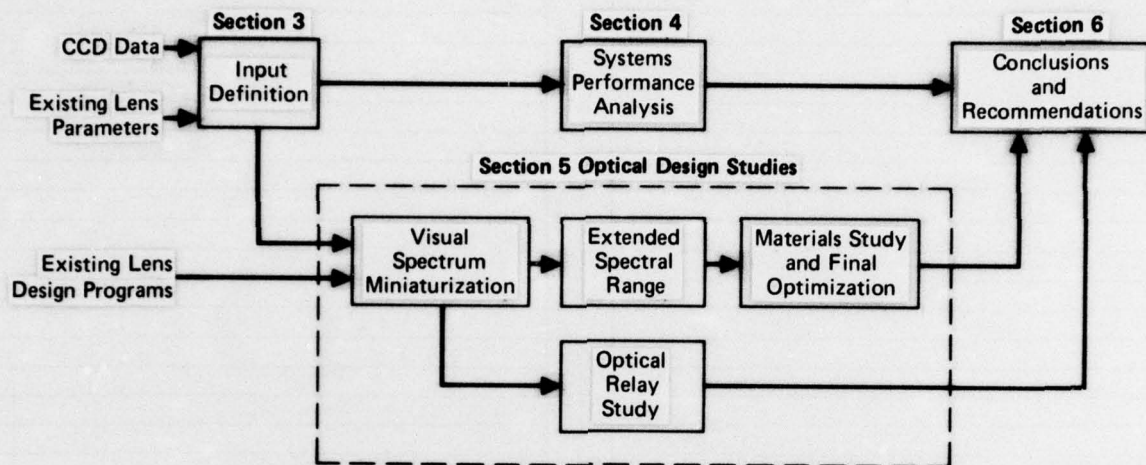


**Figure 1 Foveal Lens Miniaturization Study Approach**

### Section III

#### INPUT DEFINITION

This section summarizes studies and analyses required to define inputs before actual lens design could be initiated. These inputs are basically of two distinct types - those that are constant and will not be varied throughout the study and variables (usually referred to as tradeoff parameters).

#### A. FIXED PARAMETERS

Constant parameters are field of view, distortion, image size, focal length, and wavelength. These are defined as follows.

##### 1. Field of View

The basic RVS concept utilizing the foveal lens employs a full hemispherical coverage ( $180^\circ$ ). In order to study benefits of reducing this angular coverage, the curve of Figure 2 was generated from parametrics of our existing lens. Note only a 10% size reduction could be achieved by reducing coverage from  $180^\circ$  ( $+90^\circ$ ) to  $90^\circ$  ( $+45^\circ$ ). In view of this, the  $160^\circ$  FOV presently mechanized in our existing lens was established as a design requirement for the miniature lens.

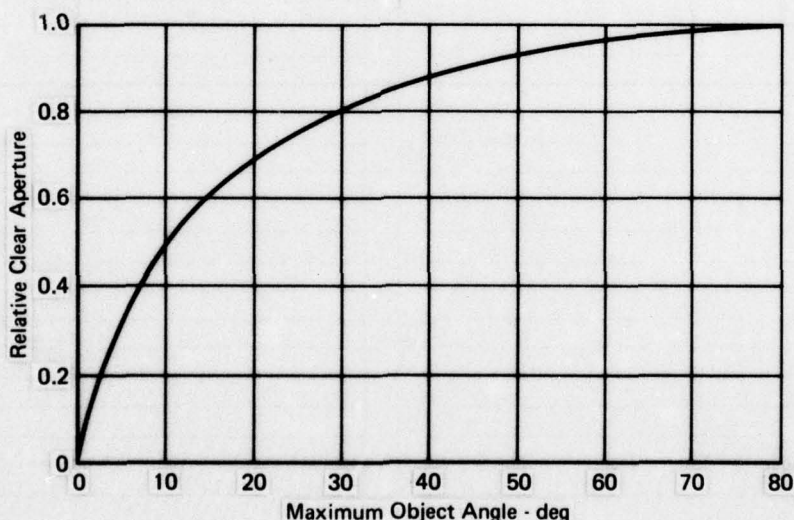


Figure 2 Lens Size as a Function of Angular Coverage

##### 2. Distortion Function

During initial design of our existing 2 inch focal length lens, a close match to the eye acuity function was used to compute the required lens distortion function. During that design effort this function was revised slightly because it was impossible to achieve the required resolution at very small field angles. This modified function is believed to be the closest match to human vision technically possible.



Both the original and revised functions are shown on Figure 3. Note how the revised function falls below the synthesized eye function at object field angles less than  $0.5^\circ$ . To see how well the lens follows design requirements, the lens design program for our existing lens was exercised to determine exactly what distortion was being achieved in the design. To supplement this, actual measurements were made on the lens by reprojecting a linear grid through the lens on a spherical surface. This image was photographed and grid line separation measured to compute the distortion function. These results are also shown on Figure 3. Over the range of measurement ( $+30^\circ$ ), the measurements agree quite well (within accuracy of the measurement technique) with the computer design predictions. Both deviate somewhat from the initial input data, but the deviation is small.

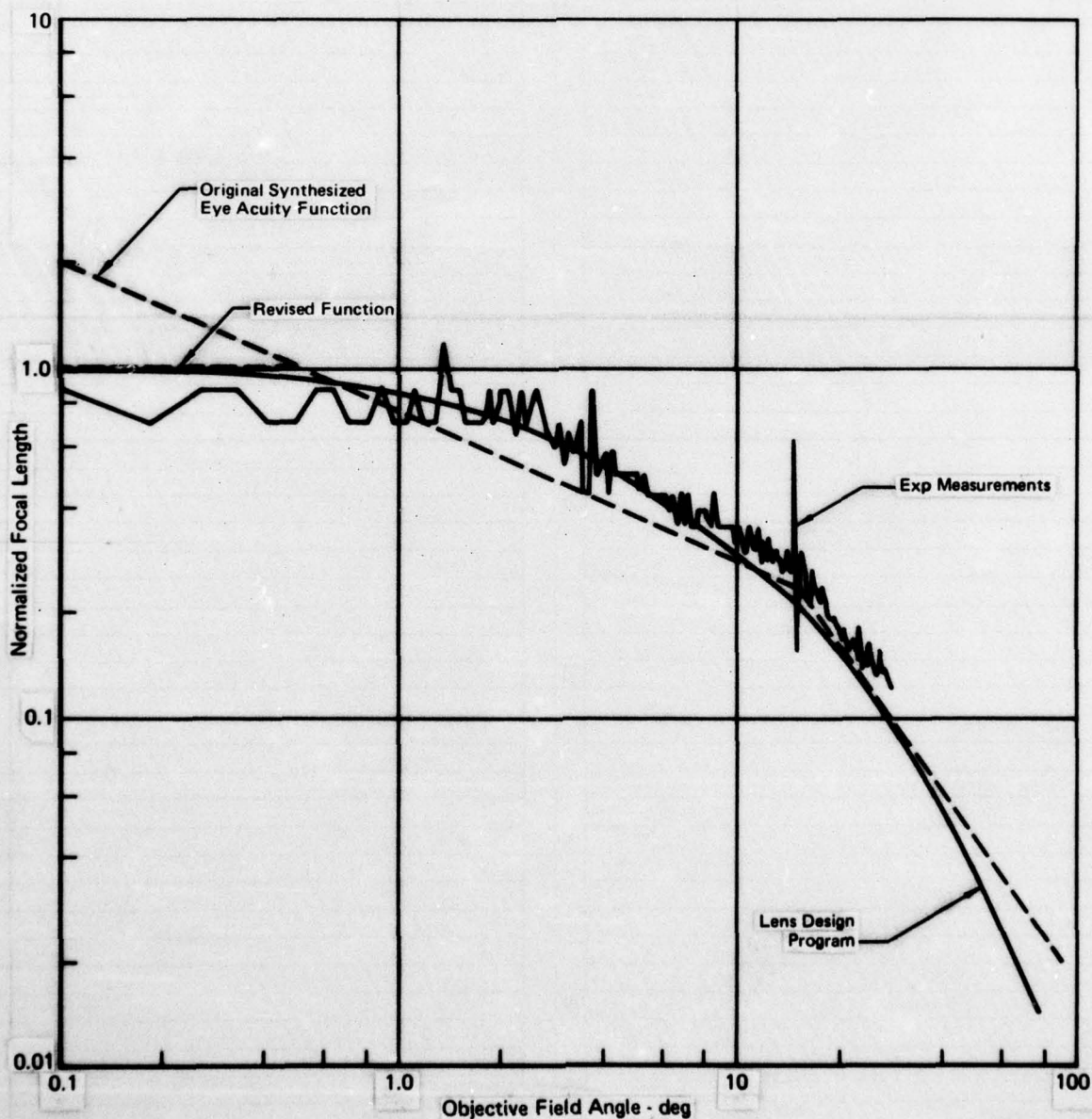


Figure 3 Lens Distortion



Based on these data it seems best to use the computer design predictions for the distortion function during foveal lens miniaturization studies. Reasons for this are:

- o The computer design function is believed to be the best compromise to the original design data. It was achieved with great difficulty and probably represents the maximum agreement achievable within practical constraints.
- o Experimental data appears to follow this data better than the original design data.
- o A lens designed to the computer predicted distortion function will be compatible with equipment designed with the existing lens. For example, a sensor fabricated with the miniature lens will be compatible with the ONR projection display system.

### 3. Image Size

The image size is governed by the CCD array geometry. As specified in the SOW, the RCA SID 51232 was used to establish image size requirements. This array requires an image size of 7.31 x 9.75 mm. In order to utilize this array in the most efficient manner, an image diameter larger than the vertical raster dimension was utilized. This measurement was arrived at as shown below.

Because of eyebrow vignetting when viewing upward and the normal lookdown interference of instrumentation controls, etc., 80° (+50 to -30) is generally considered sufficient. Referring to Figure 4 (the foveal lens transfer characteristics in terms of image height as a function of object angle), 80° total object can be achieved with 83.65% of the total image height. This layout is shown in Figure 5. To produce this geometry, the foveal lens image height must be:

$$H = \frac{7.31}{.836} = 8.74 \text{ mm.}$$

It should be pointed out that the 80° vertical viewing limit created in the attempt to utilize more of the CCD elements occurs only at zero azimuth. This increases rapidly as azimuth angles increase.

### 4. Focal Length

The on-axis focal length,  $f(0)$ , is determined directly from image height as follows. As computed in the previous paragraph, the image height for 80° is

$$h(80) = \frac{8.74}{2} \text{ mm} = 4.37 \text{ mm}$$

where  $h$  is the image height from the lens optical axis. The lens distortion equation on-axis is:

$$f(0) = 5.44 h(90)$$

Eq. (1)

where  $h(90)$  is image height at  $\theta = 90^\circ$ .

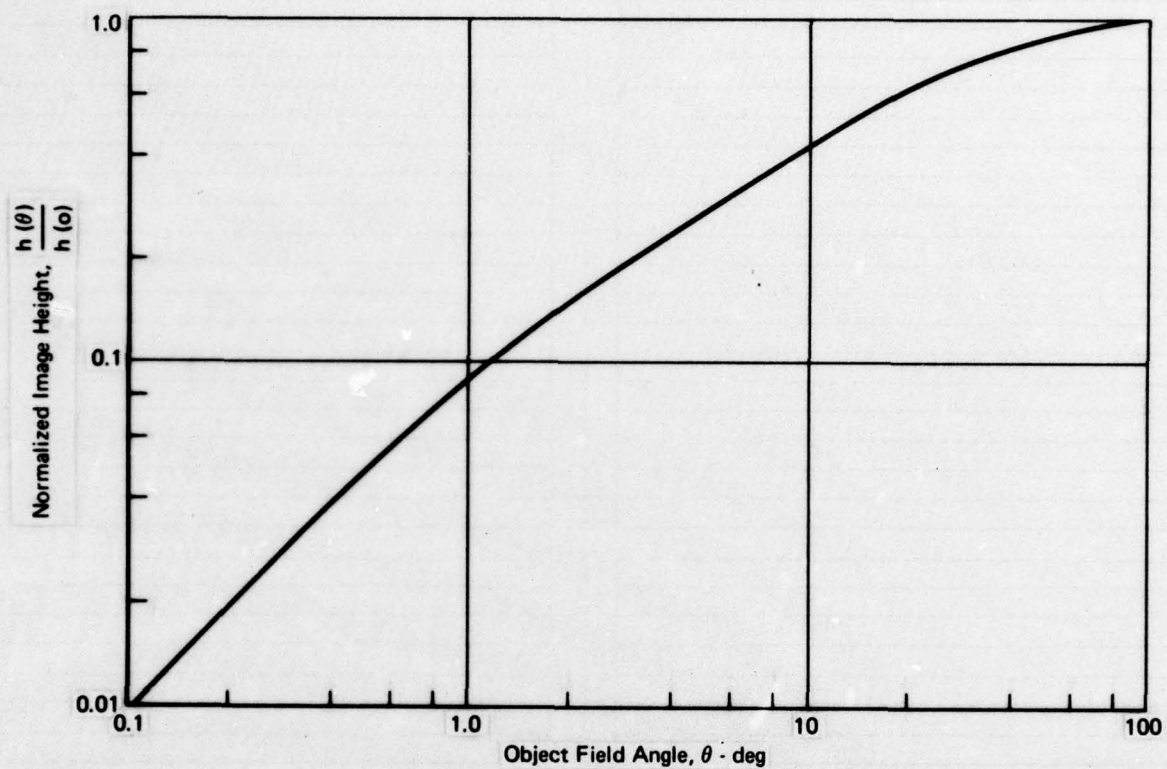


Figure 4 Lens Transfer Characteristics

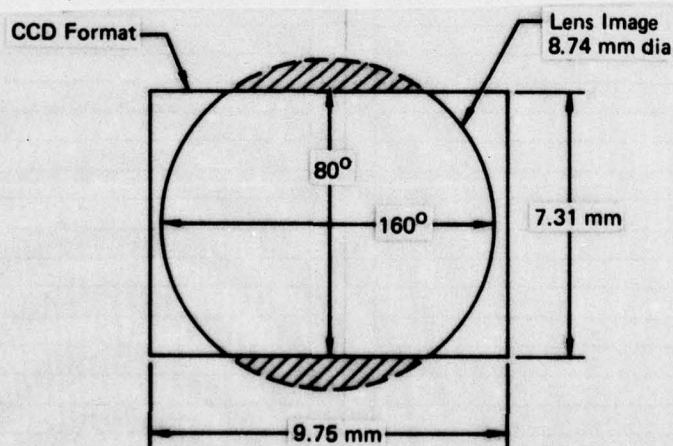


Figure 5 CCD/Lens Image Geometry

From the lens transfer characteristics (Figure 4), if

$$h(80) = .9787 h(90)$$

$$h(90) = \frac{4.37}{.9787} = 4.46 \text{ mm.}$$

Then from Equation (1)

$$f(0) = 5.44 \times 4.46 = 24.29 \text{ mm.}$$

The proximity of this value to 1 inch or 25.4 mm led us to consider pushing the focal length slightly to this value. This was advantageous because our computer design program is based on unity focal length, and scaling of results would be unnecessary. It will be seen later that minor focal length adjustments can be easily made through simple adjustments of optical components.

## 5. Wavelength

The spectral response requirements of the foveal lens are dictated by the spectral response of the CCD array. The response of the RCA unit is shown in Figure 6a. Also shown on this plot is the wavelength band used to optimize our existing lens. This spectral band was used to give best performance in the visual spectrum. It is obvious from this figure that a large mismatch exists between the lens design and CCD spectrums. Actually, optical filtering of input radiation would be required to assure maximum lens performance. The result would be greatly reduced sensitivity as is shown by the dashed line. Since our design program was working properly on the reduced spectrum, we felt it would be best to study reducing the lens size using the existing visual spectrum. After this was completed, the spectral range would then be gradually shifted to the longer wavelength region. This was initially accomplished to the region shown by the double cross-hatched region of Figure 6b. Finally, the longwave end of this spectrum was increased to 960 nm to reach the half sensitivity limits of the CCD array. With this final criteria, utilization of at least 80% of the CCD's sensitivity is assured.

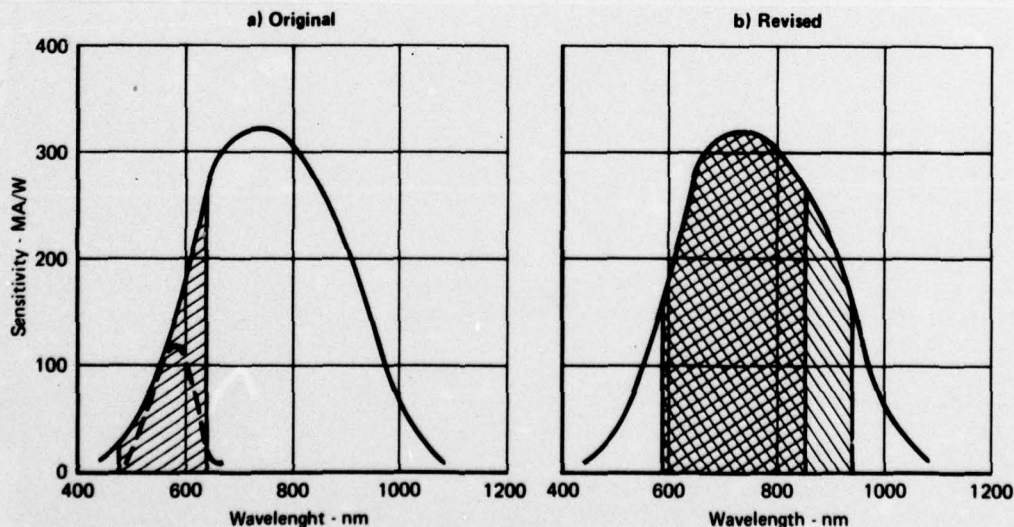


Figure 6 Lens Spectral Design Requirement - RCA SID 51232



## B. TRADEOFF PARAMETERS

Tradeoff parameters to be used in the lens design study are F/number, lens optical quality, and materials. In general, the task at this point is to establish bounds or the range of these variables.

### 1. F/Number

Obviously, lens size will be minimum with the smallest possible collection aperture or largest F/number. The task here is, therefore, to determine the largest F/number that will be acceptable in meeting mission conditions. To determine this, scene brightness requirements as a function of F/number were computed for the CCD array. In order to assure that the non-linear nature of the foveal lens does not influence photometric calculations, these equations were derived as follows: Referring to Figure 7, the luminous flux entering the Aperture D from an infinitesimal patch of ground area,  $dA_g$  is

$$F = B \omega dA_g.$$

If the surface is a lambertian radiator, this flux will, by definition, falloff with cosine of the viewing angle, i.e.,

$$F(\theta) = B \omega dA_g \cos \theta.$$

Now all the flux from  $dA_g$  will be attenuated by lens transmission,  $\epsilon$ , and fall on element of area,  $dA$ . Therefore, the illumination of the image is

$$E = \frac{\epsilon F(\theta)}{dA} = \epsilon B \omega \frac{dA_g}{dA} \cos \theta. \quad \text{Eq. (2)}$$

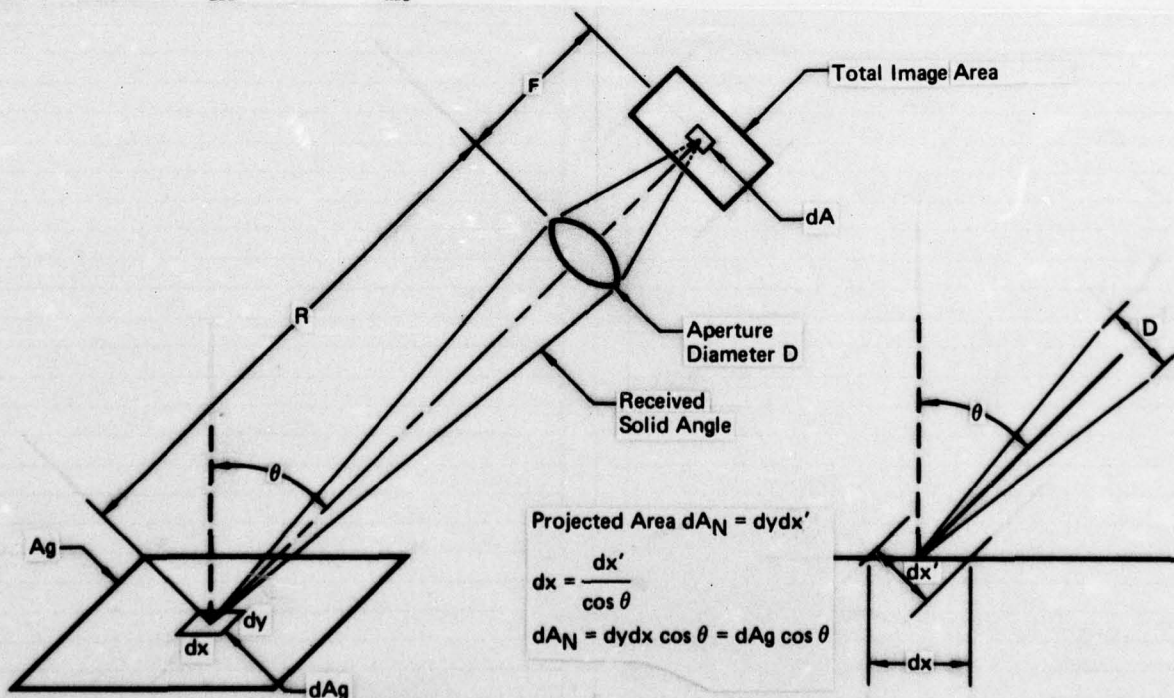


Figure 7 Sensor/Target Photometric Geometry



dA and dAg are related by simple geometry. Referring to Figure 7,

$$\frac{dA}{dA_n} = \frac{f^2}{R^2} \text{ and } dA_n = dA \cos \theta.$$

By substitution,

$$\frac{dA \cos \theta}{dA} = \frac{R^2}{f^2}.$$

Substituting this into Equation (2)

$$E = B \omega \frac{R^2}{f^2}.$$

By definition,

$$\omega = \frac{\pi D^2}{4R^2}$$

$$E = \epsilon B \frac{\pi D^2}{4R^2} \frac{R^2}{f^2} = \frac{\pi}{4} B \frac{D^2}{f^2}$$

$$E = \frac{\pi}{4} \epsilon \frac{B}{(F/No.)^2} \quad \begin{array}{l} E \text{ is in foot candles if} \\ B \text{ is in lumens/steradian - ft}^2 \end{array}$$

If B is specified in foot lamberts, by definition of this unit

$$E = \frac{\epsilon B_{FL}}{4(F/No.)^2} \text{ ft-candles} \quad \text{Eq. (3)}$$

If  $\epsilon$  is taken into account through a T number where

$$T_{No.} = \frac{F/No.}{\sqrt{\epsilon}}$$

$$E = \frac{B_{FL}}{4(T_{No.})^2} \quad \text{Eq. (4)}$$

Now for the RCA CCD under study

$$E = .1 \text{ ft-candle}$$

$$B_{FL} = .4(T_{No.})^2$$

To study how this relates to the real world, a 10% ground reflectance was assumed to obtain ground incident illumination.

$$E_g = \frac{B_{FL}}{.1} = 10 B_{FL}$$

$$E_g = 4(T_{No.})^2$$

Various  $T_{Nos.}$  were computed from this equation and plotted on the conventional earth illuminance chart, Figure 8. The following conclusions can be reached from this figure.

- o Nighttime operation cannot be achieved under any conditions unless the CCD can be made more sensitive.
- o Good daytime performance between sunrise and sunset requires a T number in the vicinity of  $T = 2.8$ . Going to  $T = 1.4$  buys very little performance improvement; while going to  $T = 5.6$  would limit operation by several hours when operating under heavy clouds.

Based on the above analysis, an F/number of 2.8 or smaller will be considered acceptable. F/number will be approximately equal to T number for the foveal lens because of the high transmission verified in the existing lens.

## 2. Lens Quality

This parameter is undoubtedly the most difficult one to quantify. It is intimately tied to F/number as it impacts on lens size. Therefore, both of these parameters must be discussed together. As a starting point, the design program for our existing lens was examined very closely to estimate how F/number and image quality influence size. The key size impact was found to be the clear aperture of the first element. Estimates of these parametrics are shown on Figure 9. They are all extrapolated from one point - our existing lens using geometrical optical theory. This should be a valid assumption for the F/number range under consideration.

Figure 9 shows that if F/2.8 is desired in a lens approximately half the size of our existing lens, an optical quality representing a 20 micron maximum spread function width will be achieved in the image plane. This figure shows that another 50% size reduction could be achieved by further reduction of optical quality to 40 microns. Obviously, the question that must be answered is exactly what optical quality is really required. This can only be resolved through some level of systems analysis. In order to accelerate entry into the lens design phase, an estimation of lens quality was made based on modulation available at the absolute resolution limit of the CCD array. There are two identifiable limiting spatial frequencies that can be easily identified for a discrete array. They are one cycle per element spacing and one cycle per two element spacings. These bound CCD performance as the maximum and minimum spatial frequencies that are theoretically possible to detect. The theoretical justification for these values and their statistical probabilities will be discussed later. They arise from relative phasing of target spatial detail to element position in the array. For the RCA CCD, which has element spacing of  $a = .0305$  mm,

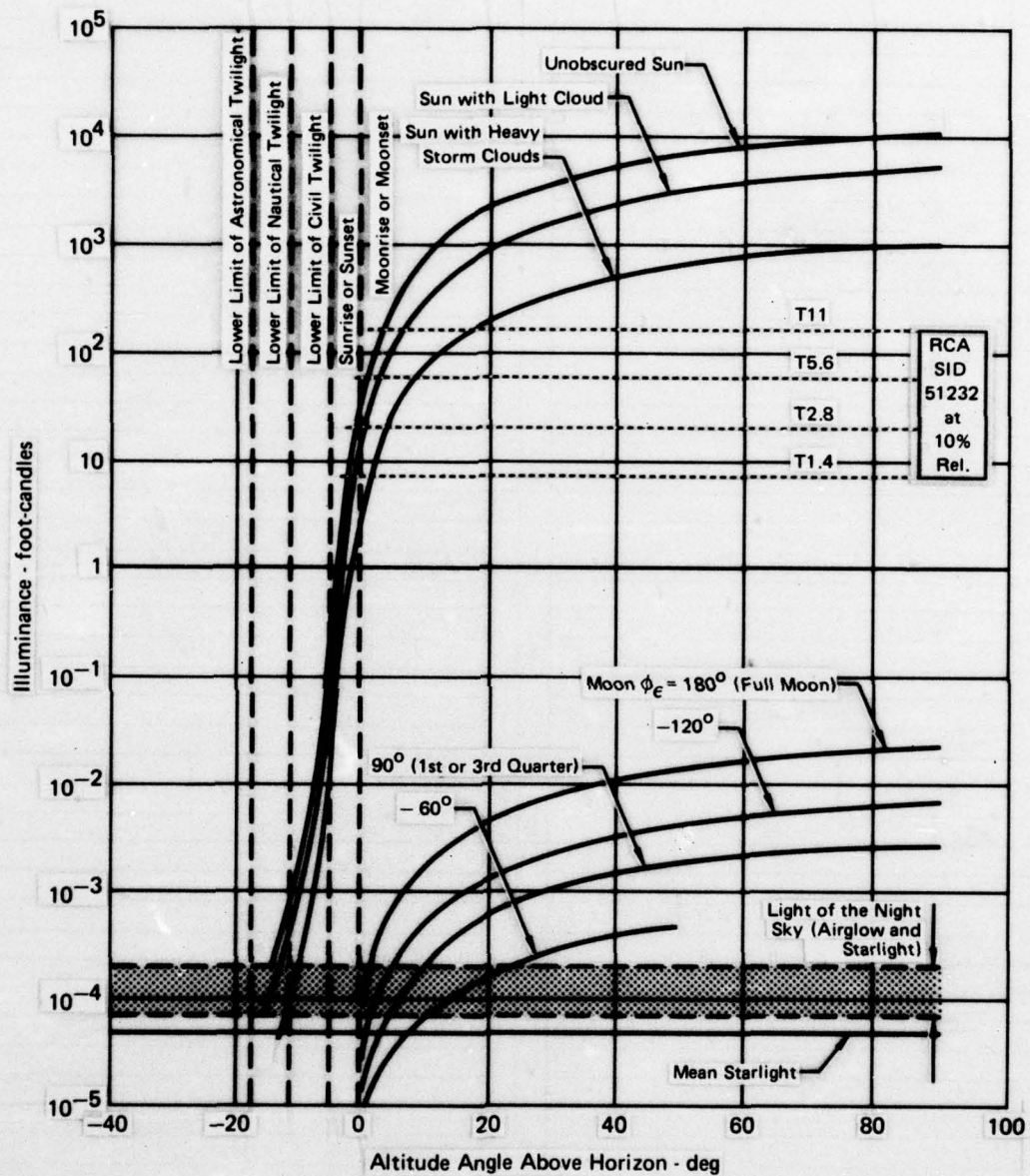


Figure 8 Earth Illuminance



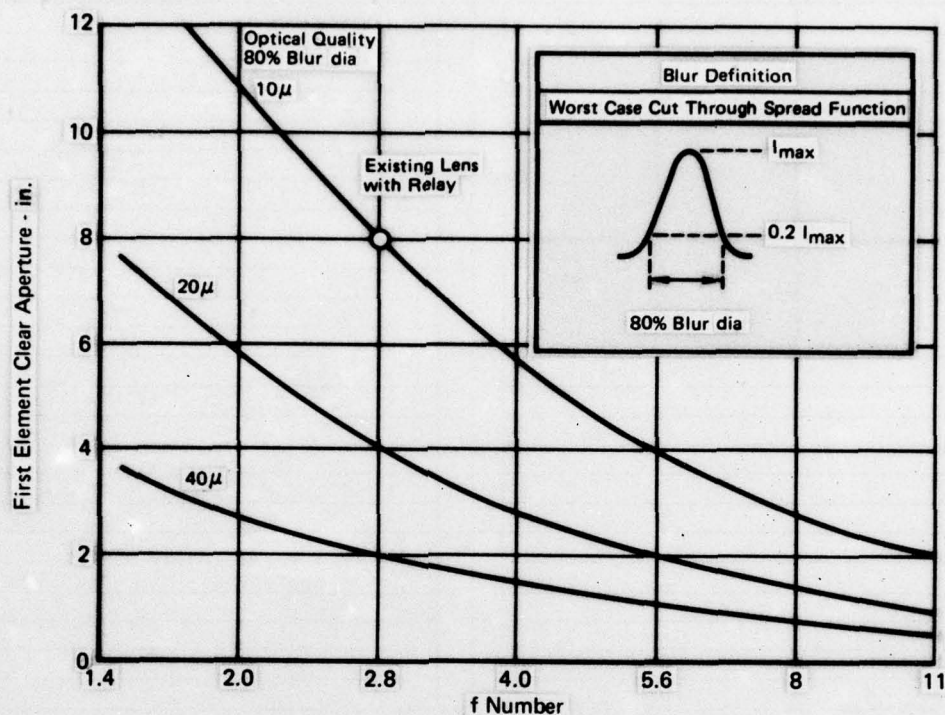


Figure 9 Theoretical Lens Size Parametrics  
Effective Focal Length = 1 in.

$$S_{\max} = \frac{1}{.0305} = 32.81 \frac{\text{cycles}}{\text{mm}}$$

$$S_{\min} = \frac{1}{2 \times .0305} = 16.40 \frac{\text{cycles}}{\text{mm}}$$

The lens MTF is estimated as follows. Review of blur plots indicate the worst case spread function cross sections are very nearly Gaussian in shape, i.e.,

$$I(x) = I_m e^{-1/2 \left(\frac{x}{\sigma}\right)^2} \quad \text{Eq. (5)}$$

The value of sigma ( $\sigma$ ) required to define this equation can be computed from our 80% blur circle diameter as follows. (See Figure 9.)

$$D_{(80)} = 2x \text{ (when } I = .2 I_m \text{)}$$

From Equation (5),

$$.2 I_m = I_m e^{-1/2 \frac{D_{80}^2}{2\sigma^2}}$$

Solving for sigma

$$\sigma = \frac{D_{80}}{3.59} \quad \text{Eq. (6)}$$

The lens minimum MTF is derived from the maximum width spread function by taking the Fourier transform of Equation (5). The result is

$$\tau(S) = e^{-2\pi^2 \sigma^2 S^2} \quad \text{Eq. (7)}$$

where  $\sigma$  is defined by Equation (6), combining Equations (6) and (7),

$$\tau(S) = e^{-1.532 D_{80}^2 S^2} \quad \text{Eq. (8)}$$

Now studying this at the maximum detector spatial limit

$$\tau(S) = e^{-1.532 D_{80}^2 (32.81)^2} \quad (\text{Note: } D_{80} \text{ must be in mm})$$

$$\tau(32.81) = e^{-1649 D_{80}^2} \quad \text{Eq. (9)}$$

For the minimum spatial frequency, the equation is

$$\tau(16.40) = e^{-412 D_{80}^2} \quad \text{Eq. (10)}$$

Equations (9) and (10) are plotted in Figure 10. This figure indicates that a lens requirement of about  $10\mu$  would be desirable. A modulation between 85 and 95% would be available regardless of relative phasing of target/detector element detail. For an F/2.8 lens, Figure 9 shows that an 8 inch clear aperture lens would be required. This fact led us to consider a  $20\mu$  optical quality. There are several reasons for this besides the lens size reduction, i.e., the 4 inch clear aperture it produces. First and most important, past design experience has demonstrated that the worst case spread functions occur in the meridional plane only and in only one or two narrow angular zones. In all other angular zones and in the tangential directions, performance is two to five times better than the worse case value. Considering this, a "not to be exceeded" blur specification of  $20\mu$  would probably assure that 90-98% of all measurements in the image plane are better than  $10\mu$ . Even at the worse case points, modulation would be between 50 and 85% (a creditable value in the radial directions), while tangential measurements at the same point will yield modulations in the 85-95% range or better.

This rationale was utilized to justify a  $20\mu$  blur specification in initial design efforts. Work has continued in this area throughout the entire contract. This work will be discussed later in Sections 4 and 6.

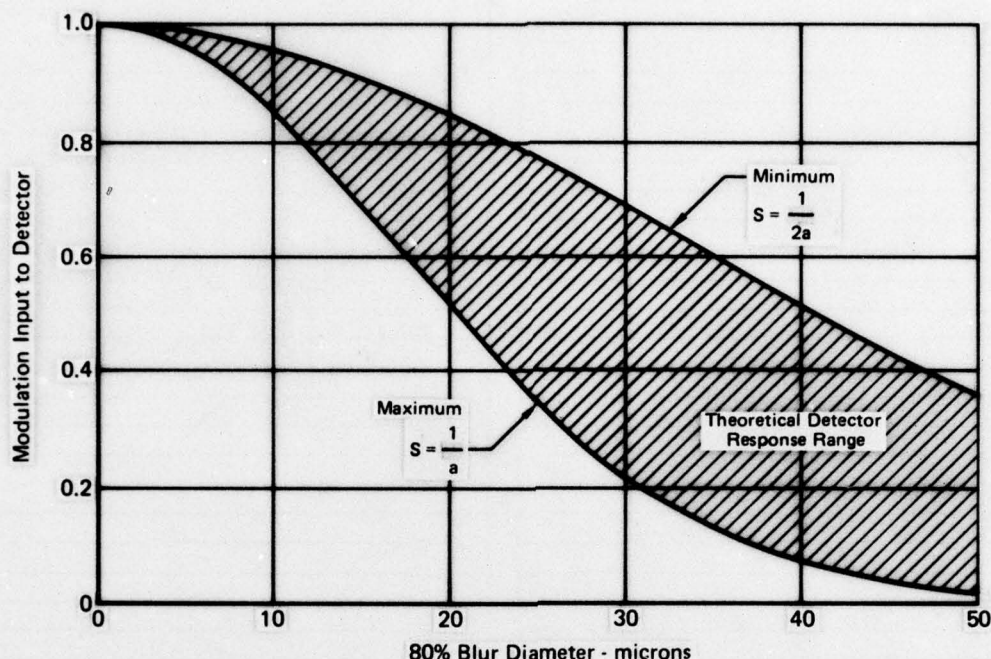


Figure 10 Modulation at Lens Image for Critical Detector Response Frequencies  
( $a = 0.0305\text{mm}$ )

### 3. Optical Materials

Materials considered vary from the complete family of optical glasses to optically and mechanically acceptable plastics. These tradeoffs apply primarily to the aspheric elements because the small spherical elements can be fabricated more cheaply from glass (Reference 1). In addition, the wide range of dispersions and indices of refraction available in glasses assists chromaticization of a lens using plastic aspherics. Some additional materials considerations are discussed below.

- o Glass Elements - Glass types for the elements, after their approximate index and dispersions are established, are then specifically selected for their physical and chemical properties. High resistance to straining and climatic variations, internal transmittance, and good optical properties are considered when identifying specific glass types.
- o Plastic Elements - A detailed analysis for the specific fabrication approach of the plastic spline elements has not been made. General fabrication approaches for plastic elements are as follows:

Plastic elements can either be fabricated by casting, molding, or machining.

- a. Casting is normally reserved for large (in volume and size) elements. Environmental conditions for the curing area are important, and throughput is low due to long curing time. Fabrication rate can be increased with additional molds.



- b. Injection and compression are the methods used in the molding process. For compression molding, the plastic is in powder or pellet form placed between heated dies in a press. Cycle time in the press is relatively long coupled to in-die curing time after removal from the press. Injection molding uses the plastic in liquid form injected under high pressure into a mold. Cycle time is relatively short. Satisfactory injection molding of large elements is somewhat difficult to achieve.
- c. Machining of plastic elements is an easy process through use of numerically controlled machines. Polishing of the elements is more difficult than with glass. There really is no advantage to plastic elements when the machining process is used.

The major advantage in utilizing plastic is in the ability to produce low cost replications from an expensive aspheric mold. For spherical shapes, large production runs have to be made before the cost of the plastic elements are below their equivalent glass types.

To achieve reasonable performance levels, detailed attention has to be given to the thermal and physical properties. Index variations with temperature of 0.0001/deg C is one to two orders of magnitude greater than glass. Compensation techniques through thermal sensitive spacers within the lens mount are required.

The physical properties such as shrinkage and stability have to be considered when selecting specific plastic types for the elements.

Anti-reflection coatings can easily be applied with some care, although the coatings are soft as opposed to the hard coatings available on glass.

- o Cost Considerations - The anticipated number of lenses required will dictate the approach of using all glass elements as opposed to a hybrid plastic and glass combination system. The cost of molds and molding process will have to be traded off with glass fabrication costs versus number of lenses required. Fabrication of spherical glass elements can be accomplished at relatively high volumes before a savings through using spherical plastic elements is realized (Reference 1).

## C. PRACTICAL DESIGN CONSTRAINTS

### 1. Element Shape

The foveal lens achieves its imaging characteristics through the use of unconventional aspheric spline elements. The spline elements, which have rotational symmetry, cannot be generated by "standard" optical shop techniques. The extreme asphericity dictates the use of tape or pantagraph type controlled grinding machines. Conformance to required surface figure has to then be established by physical profile measurements. The smaller the element diameter, the tighter the tolerance requirements. This makes both fabrication and measurement more difficult.

## 2. Element Sizing

For the miniaturization of the original foveal lens, problems encountered during the fabrication of the "full scale" lens determined some of the basic size constraints for the study. Performance data from the first foveal lens indicated that the design could be scaled to one-half size while still maintaining adequate resolution or acuity. This proved not feasible due to the difficulties encountered while trying to grind and polish the last element ahead of the image plane. This element (number eight) has a spline/convex shape and would have a diameter of only 0.35 inch. In our existing lens this element has a diameter of 0.7 inch. Even this size was found to be marginal for generation on a tape controlled machine; therefore, the fabricator elected to hand figure the element. As a result, the measurements show that the two elements (for our two lenses) are different from each other though still within stipulated fabrication tolerances. The tighter tolerances required of smaller elements would definitely be impossible to achieve.

Subsequent discussions with the fabricator have resulted in an opinion that spline elements in the 0.7 inch diameter area or larger can be generated without resorting to hand figuring. This is also believed to be a reasonable limit for plastic elements because mold fabrication has identical problems.

Based on these points, the minimum size for any spline elements was limited to 0.7 inch. This inherently establishes a minimum focal length for the basic foveal lens of about 2 inches. A 2/1 optical relay will, therefore, be required to achieve the required effective focal length of 1 inch.

## Section IV

### SYSTEMS PERFORMANCE ANALYSIS

As mentioned previously, a systems analysis effort was run concurrent with the optical design effort in order to verify or modify lens quality requirements. This effort is described below. The non-linear nature of the RVS video requires caution in application of conventional sensor performance modeling theory. The measure of merit of the RVS as a sensor is how well its display output, presented to the observer, is a true representation of its optical input. Since the RVS is a unity magnification device, objects are presented to the observer in the same angular perspective that they are received by the sensor. With angular subtense of objects guaranteed by the inherent geometry of the RVS, degradations will appear only as contrast or modulation losses in the displayed image. This measure of merit can be obtained by the Modulation Transfer Function (MTF) of the RVS system. Figure 11 shows significant MTF's that are involved in the RVS system. This representation is somewhat different from conventional TV systems in the non-linearity at input and output ends of the system, i.e., the distortion function,  $F(\theta)$ , representing the focal length change as a function of the object field angle,  $\theta$ .

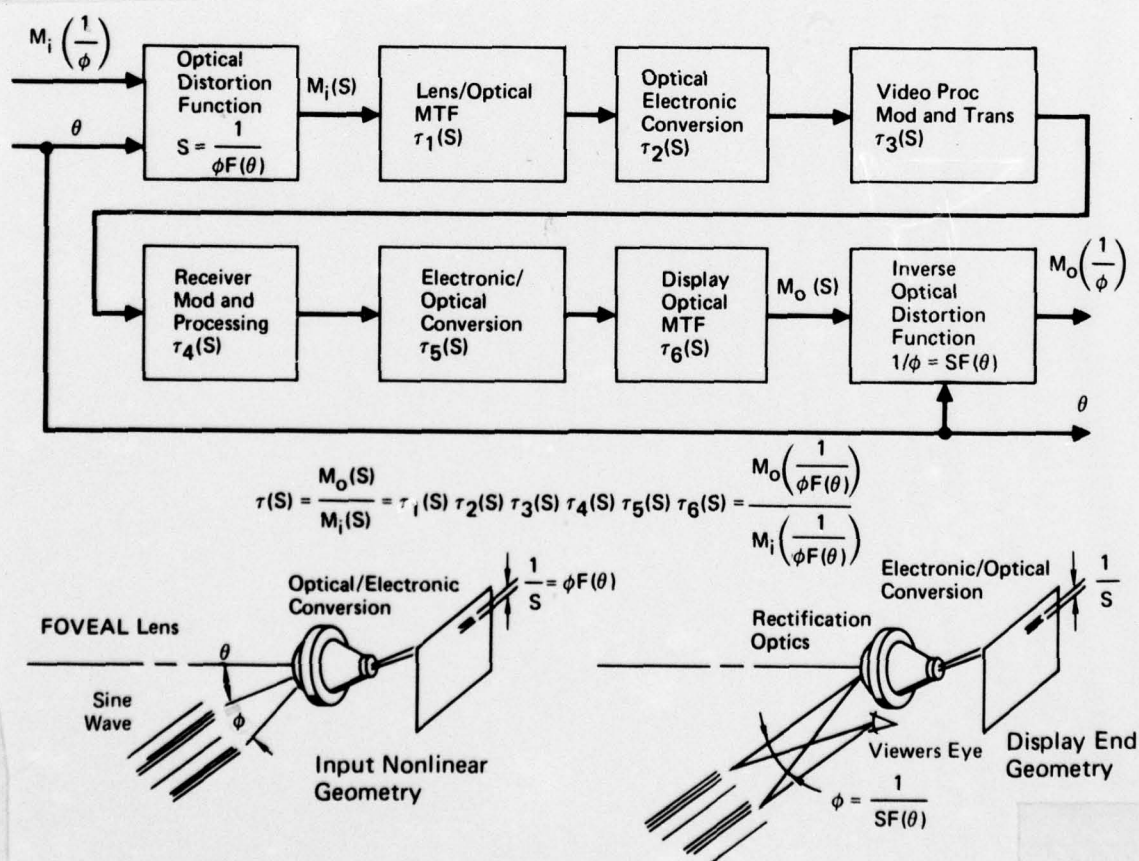


**Figure 11 General RVS Optical Transfer Function Representation**



## A. THE SENSOR LENS

At the input end, the foveal or non-linear lens has the function of converting object angles,  $\phi$ , to a linear focal plane through its focal length function,  $F(\theta)$ . On Figure 11 a sinusoidal object distortion is shown with angular subtense,  $\phi$ , for one cycle. This is related to conventional spatial frequency in the focal plane by the apparent lens focal length,  $F(\theta)$ , i.e.,

$$S = \frac{1}{\phi F(\theta)} \quad \begin{array}{l} \text{cycles/inch or cycles/mm} \\ \text{(depending on } F(\theta) \text{ units)} \end{array} \quad \text{Eq. (11)}$$

Note that the translation from  $\phi$  to  $S$  will vary with the angular separation the object appears from the lens optical axis,  $\theta$ . Progressing to the next element of Figure 11,  $\tau_1(S)$  yields modulation loss caused by the lens. Since the lens is designed with constant resolution in its focal plane, its MTF in spatial frequency,  $S$ , terms will be independent of object angle,  $\theta$ . The same is true of all other elements in the MTF chain up to final object being viewed by the observer. Here the translation into angular space is the reverse of the input end, i.e.,

$$\phi = \frac{1}{S F(\theta)} \quad \text{Eq. (12)}$$

Since the overall MTF,  $\tau(S)$ , is independent of  $\theta$ , it will yield system degradation for any field angle. This is a very significant observation in that, once the system MTF,  $\tau(S)$ , is determined, system performance at any field angle,  $\theta$ , can be instantly and simply determined through the distortion function,  $F(\theta)$ . It is only when relating to ground objects or to the observer that this non-linear relationship must be employed. For example, to determine system performance of a ground target having spatial frequency  $K$  at range  $R$  and at field angle  $\theta$ ,  $\phi$  is simply determined as

$$\phi = \frac{1}{KR}.$$

This is then converted to  $S$  by

$$S = \frac{1}{\phi F(\theta)} = \frac{KR}{F(\theta)} \quad \text{Eq. (13)}$$

The modulation of this object, as seen by the observer, is simply the received modulation (the target/background modulation degraded by the atmosphere) times the MTF at spatial frequency,  $S$ , i.e.,

$$M_o = \tau(S) M_1 \quad \text{Eq. (14)}$$

The observer's capability to see this object, however, is a complex subject that will be addressed after system MTF's are fully defined. Starting from the sensor optical input, the optical distortion function is  $F(\theta)$  as discussed in Section 3.1 and shown on Figure 3. Approximate equations are:

$$F(\theta) = F(0) \quad \text{for } 0 < \theta < .515$$

$$F(\theta) = .755 F(0) \theta^{-.423} \quad \text{for } .515 < \theta < 15$$

$$F(\theta) = 10.27 F(0) \theta^{-1.387} \quad \text{for } 15 < \theta < 90^\circ$$

With  $F(\theta)$  defined, the next function on Figure 11 is the lens MTF. This can be easily derived from lens design requirements. These are in terms of point spread functions at its focal plane, and the same value applies anywhere on the image area. The worst case MTF can be obtained by taking the Fourier transform of the specified worst case spread function as previously discussed in Section 3.2 and is defined by Equation (8), i.e.,

$$\tau_1(s) = e^{-1.532 D_{80}^2 s^2}$$

#### B. THE OPTICAL/ELECTRONIC CONVERSION

Based on USAF recommendations, we utilized the RCA SID 51232 as the conversion device for our model. Initially, we utilized their brochure "typical" MTF as  $\tau_2(s)$ . We later became concerned as to the statistical predictability of this MTF and conducted our own analysis to determine theoretical limits and statistical distribution of this type discrete image extraction system. The analysis is summarized below. Details of the analysis is presented in Reference 2.

Our reasons for concern can be shown through several simple figures. Figure 12 shows basic elements needed to study the problem. Here the scene is imaged on the array of discrete detector elements at the lens image plane. Since each detector generates an electrical output proportional to the energy it receives, the array output is essentially a sample data system as shown in Figure 13. When working with MTF theory, we are concerned with relative outputs of the elements when imaging a sinusoidal pattern. This geometry is shown in Figure 14. The problem with this type imaging system is shown in Figure 15. Here a sine wave with a spatial half period equal to the element spacing is shown in two phase positions.

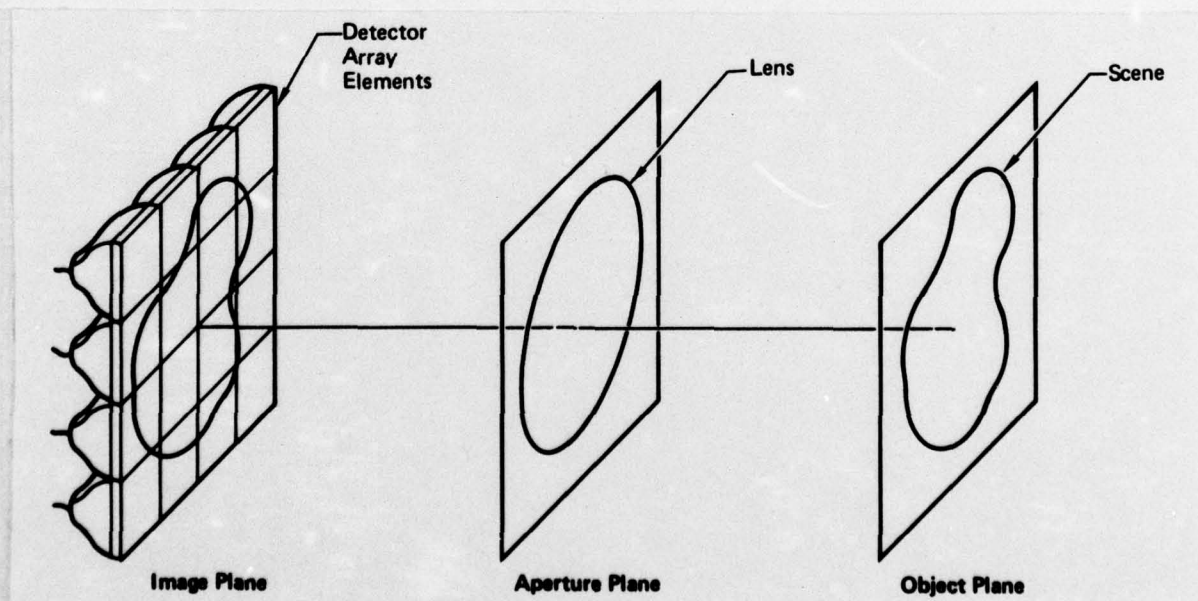


Figure 12 Array Detector Geometry

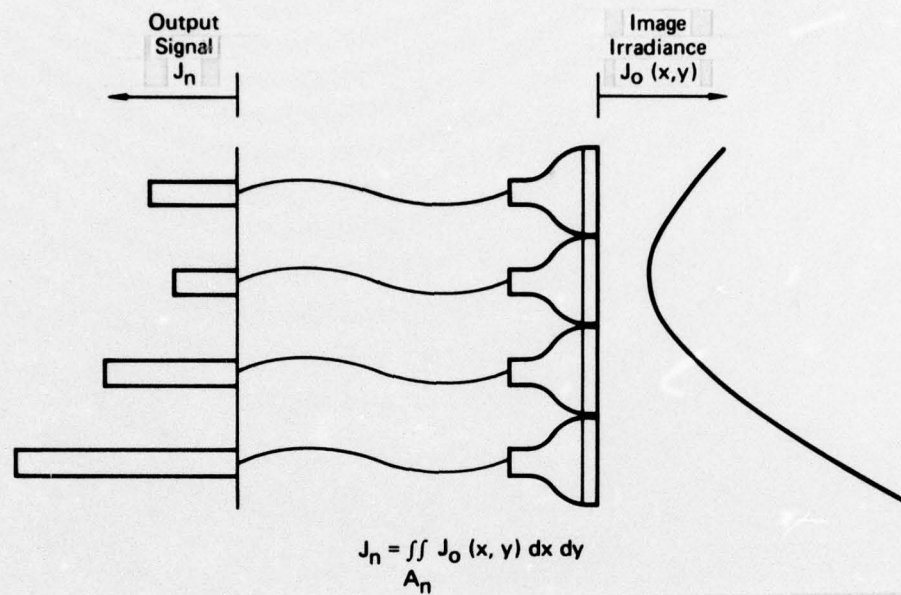


Figure 13 Input/Output of Array Elements

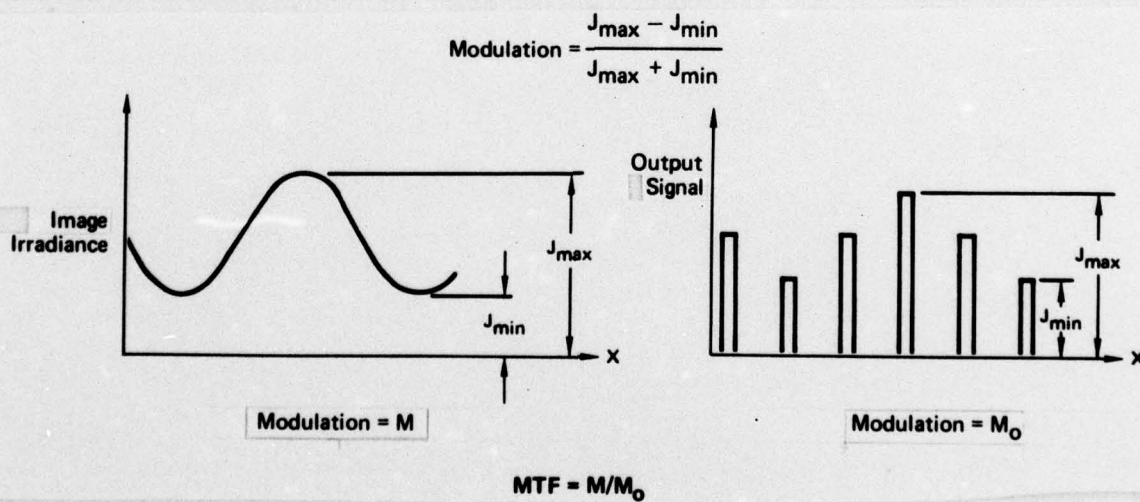


Figure 14 Modulation and the Modulation Transfer Function (MTF)



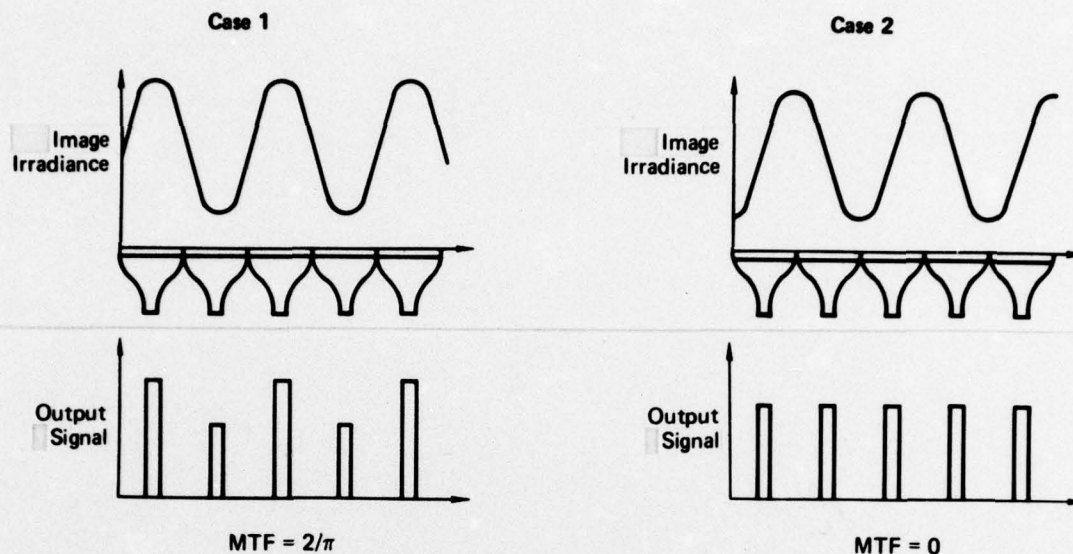


Figure 15 Variation of MTF with Phase Angle

In Case 1 a large modulation in electrical output is obtained, while in Case 2 no output is produced. Obviously, this phase should be handled as a random input variable, and our primary interest is in the statistics of the output modulation. This theory is developed in Reference 2. A sample of the kinds of data derived for the RCA array in that reference is shown in Figure 16. This is the probability density distribution of modulation at two different spatial frequencies. Note that discrete maximum and minimum limits exist. This is true of all spatial frequencies as shown on Figure 17. Here the maximum, minimum, and average modulations at all spatial frequencies are shown. In practice, the actual MTF can be anywhere between these limits.

It is interesting to compare these statistically derived data to the conventional method for handling discrete detectors - the Fourier transform of a square spread function. This comparison is made on Figure 18. Note that the conventional method of representing an array MTF is considerably optimistic, i.e., a very low probability exists that it could be realized. The average theoretical MTF was selected for our systems analysis. This is the mean MTF, which will be exceeded approximately 50% of the time.

### C. REMAINING MTF'S $\tau_3$ TO $\tau_6$

The remaining MTF's of Figure 11 are impossible to define at this time. However, the following rationale was used to make preliminary analysis possible.

- o No video processing is assumed, and no degradations due to modulation, transmission, reception, and demodulation are assumed. This implies  $\tau_3$  and  $\tau_4 = 1$ .
- o It is assumed that display resolution performance far exceeds the requirements so that  $\tau_5$  and  $\tau_6 = 1$  over the spatial frequency range of interest. Since size/space and cost requirements are not very stringent for the remote display, this seems like a reasonable assumption at this point.

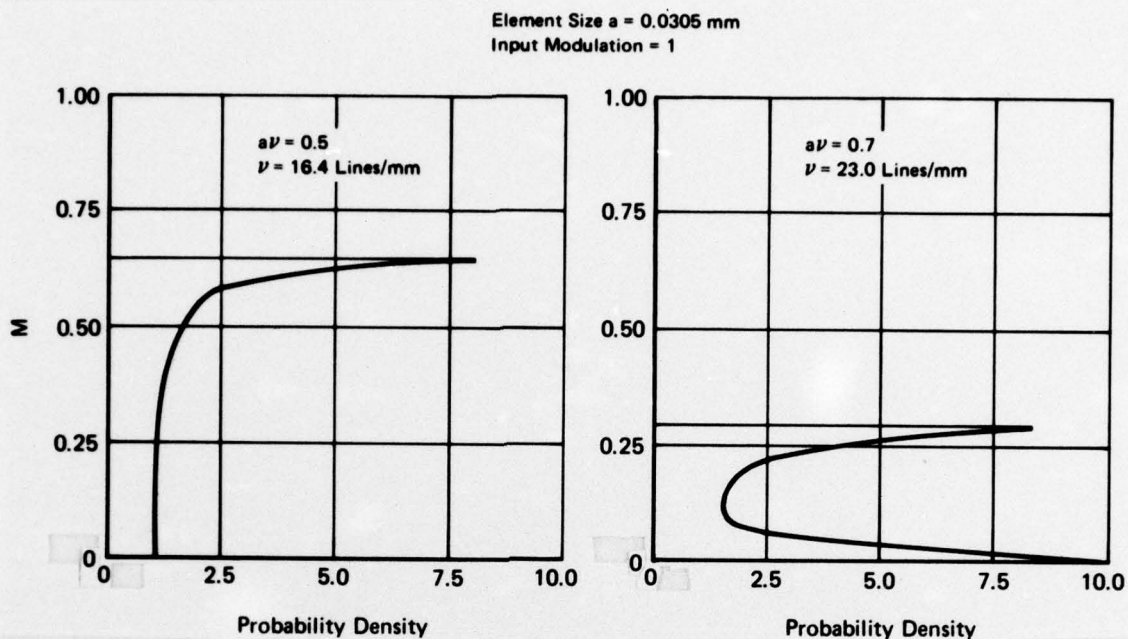


Figure 16 Probability Density Function of Modulation - RCA SID 51232

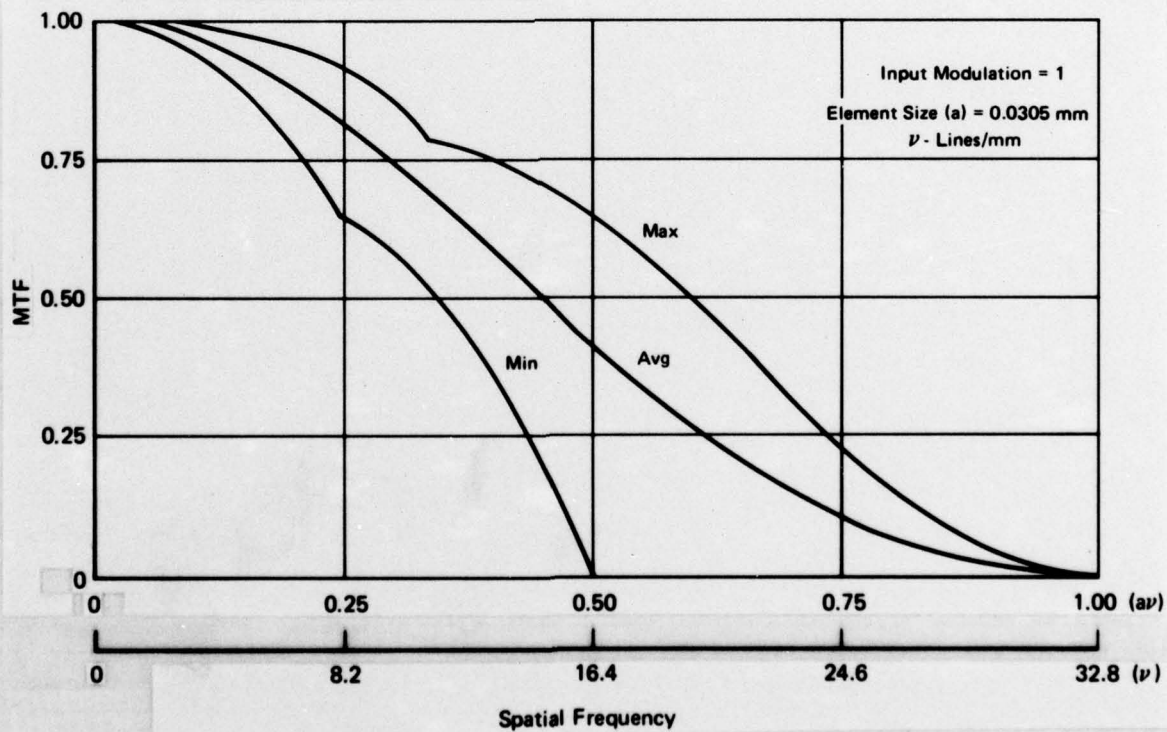
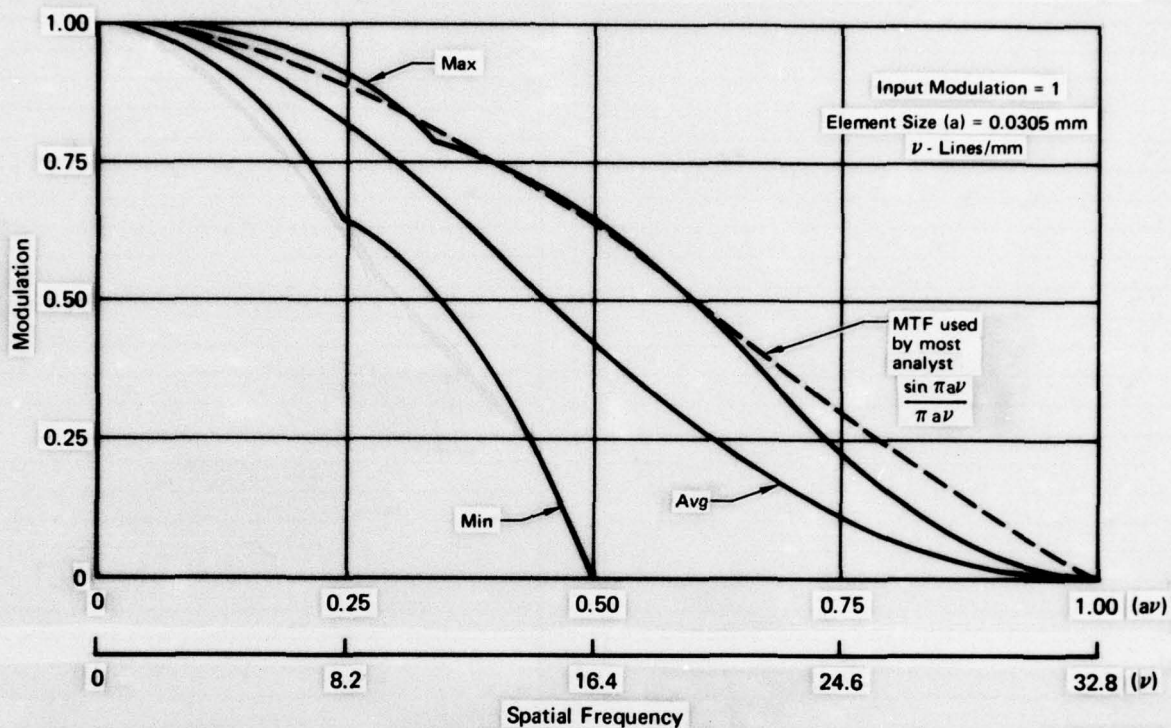


Figure 17 Maximum, Minimum, and Average MTF - RCA SID 51232



**Figure 18 Theoretical MTF Compared to Conventional Representation Method  
RCA SID 51232**

Utilizing the parameters defined above, the overall MTF is:

$$\tau(S) = \tau_1(S) \tau_2(S)$$

This function describes the modulation loss in the final displayed image to the viewer. If the viewer is to resolve this displayed image, it must have sufficient angular subtense, contrast, brightness, and signal to noise ratio. The first of these can be determined from spatial frequency,  $S$ , and the lens distortion function,  $F(\theta)$ , i.e.,

$$\phi = \frac{1}{S F(\theta)}$$

Contrast is available from the MTF, i.e.,

$$M_o = M_i \tau(S).$$

Brightness is a characteristic of display capability; it was carried as a variable in the analysis. The RMS noise in the displayed image arises primarily from system electronic noise and sensor CCD element non-uniformity. A value of 0.4% was extracted from RCA data on the CCD.



#### D. OBSERVER PERFORMANCE

Observer capability in terms of the above parameters was derived from the Statistical Detection Theory developed by H. A. Ory of Rand Corporation (Reference 2). In this document, statistical detection theory of threshold visual performance is developed in which the neural excitation noise results from both target and background luminance. Detection occurs if the number of excitations resulting from observation of the fluctuating target and background luminance exceeds programmed decision criterion. This work was developed for detection of a blob from a uniform background and was verified by the Tiffany data on visual thresholds. It must be modified substantially for the sinusoidal target of MTF theory. This is accomplished as derived in the work of Reference 2. The resulting equation is plotted in Figure 19 for three levels of display brightness. Note the trends are correct and magnitudes close to what experience would dictate. The penalties of low display brightness are clearly seen. For example, if  $M_o$  is about .0125, 2.5 min arc resolution can be obtained from a 10 ft-lambert display; while only about 12 min arc could be obtained from a 1 ft-lambert display.

System noise was included by computing the rms of the visual threshold functions with system rms noise. A noise value of .004 was used for this purpose.

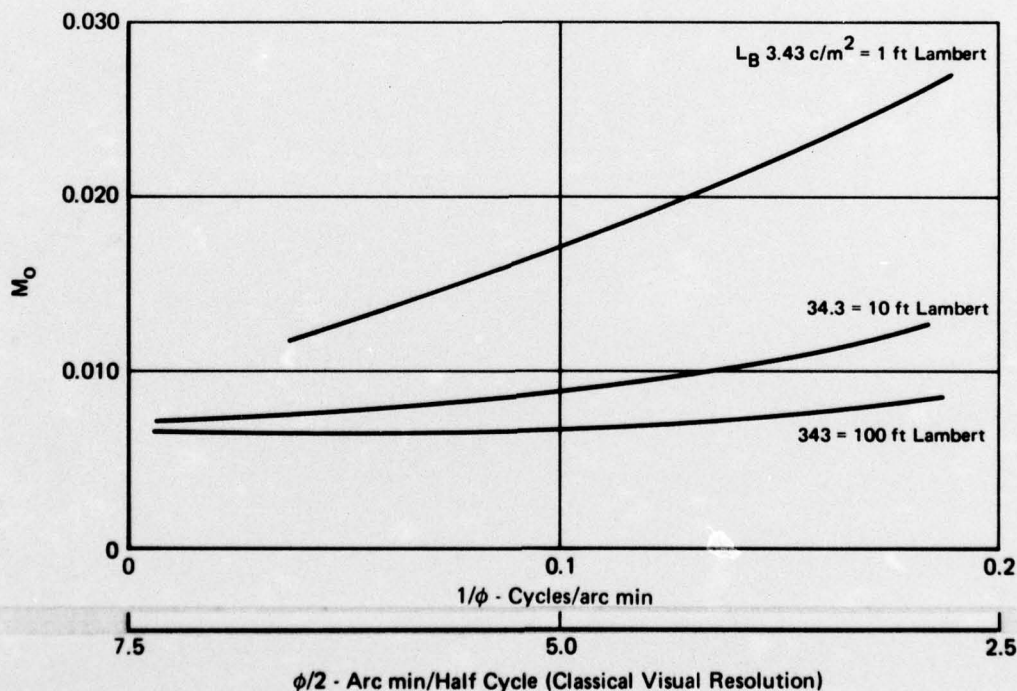
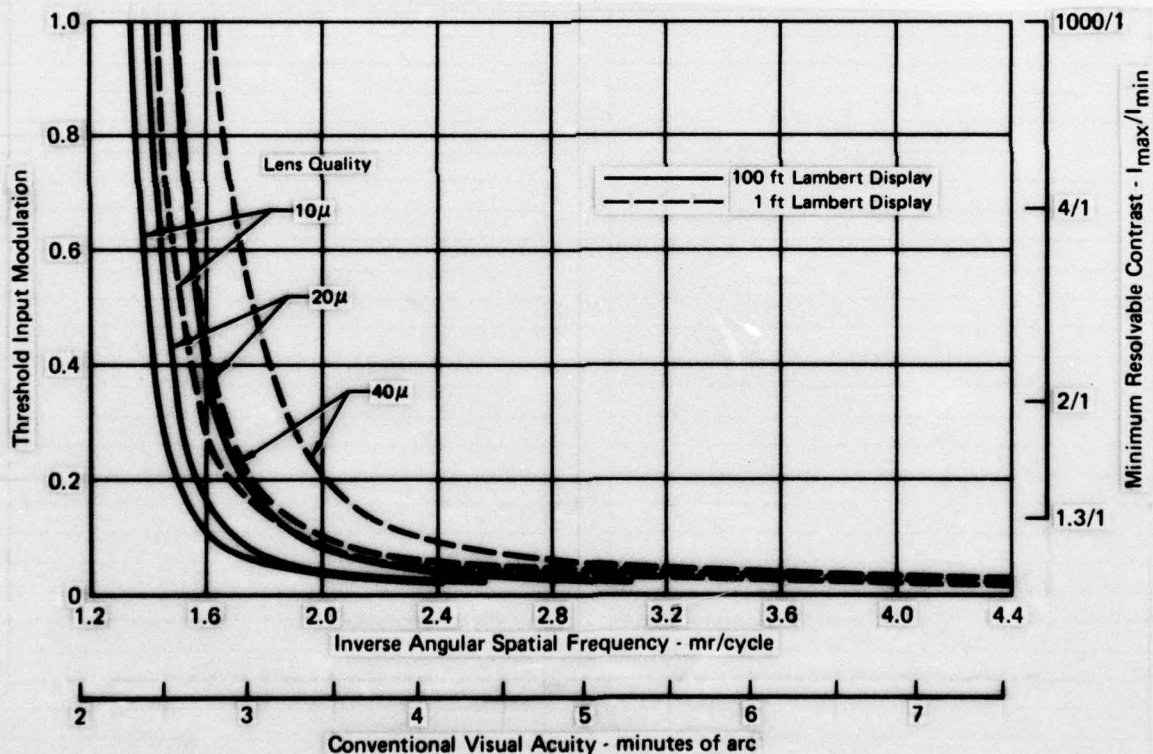


Figure 19 Visual Threshold as Functions of Display Brightness and Resolution

## E. RESULTS

Using the analytic model discussed above, the effects of lens optical quality was examined for several levels of display brightness. Figure 20 shows results for two levels of display brightness - 100 ft-lamberts and 1 ft-lambert. By locating the spatial detail of interest on the x-axis, the sensor input modulation or contrast required for detection of this detail is read from the y-axis. The following conclusions can be reached from this figure.

- o The 20 $\mu$  lens quality estimated early in the study was a good choice. Improving quality to 10 $\mu$  buys very little improvement, while reducing quality to 40 $\mu$  causes significant degradation at low contrast. In addition, a 40 $\mu$  lens could not support either image magnification or a better CCD if these features were required in the future.
- o Good display brightness is even more important than lens quality in achieving good performance.



**Figure 20 Minimum Resolvable Contrast - 1 In. Focal Length Lens, RCA SID 51232 Sensor**

## Section V

### OPTICAL DESIGN STUDIES

Before beginning detailed discussions of this phase of the effort, some reiteration of certain input data is in order. First, a constraint of 2 inch minimum focal length is required of all foveal lens configurations for reasons discussed in Section 3.3. Therefore, a 2/1 optical relay will be required to achieve the desired 1 inch effective focal length. Design feasibility of this relay is also considered part of the optical design studies presented in this section.

The work described in this section proceeds along the lines of Figure 21. This is a repeat of the lower portion of Figure 1 with the addition of "sample configuration" identification letters. These sample configurations represent significant stages in the several hundred individual computer runs that were made during the study. These selected examples are fully identified in Table 1. Reference to this table and Figure 21 will be of assistance in the following discussions.

To give the reader an appreciation for the volume of data generated during this study, one computer run has been reduced and is enclosed as Appendix A.

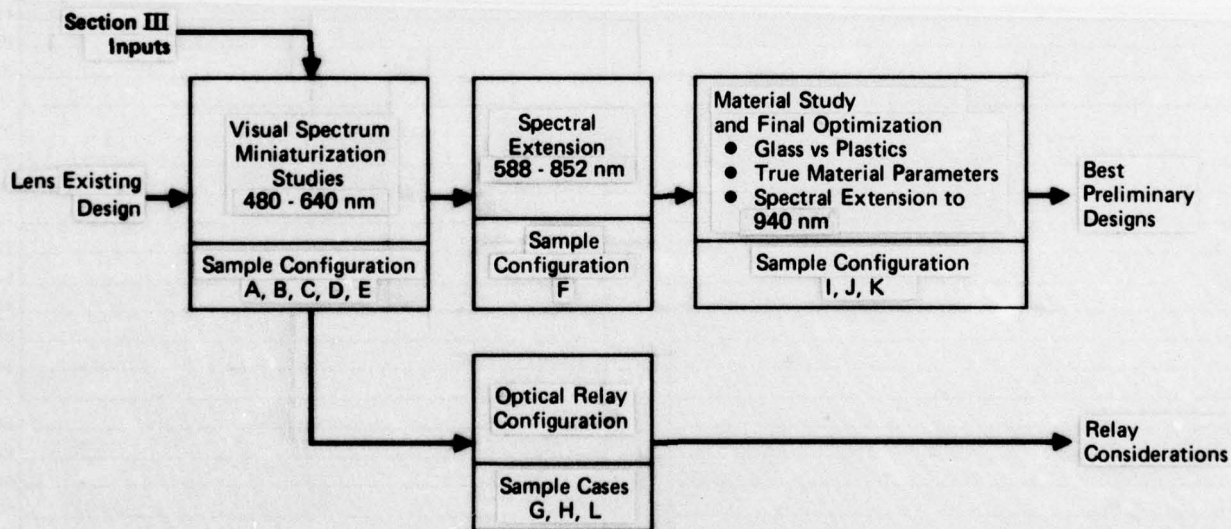


Figure 21 Design Study Approach

#### A. MINIATURIZATION IN THE VISUAL SPECTRUM

The optimization process started with the original foveal lens, Optical Configuration (A), on Table 1. For the initial study sequence, the same spectral band (480 nm to 640 nm) and materials (SK 16 and F2) were utilized, and the first element and pupil diameters were reduced by 50%. The rescaling of the original design was basically a manual operation involving multiplication of the numerical aperture, spline endpoint heights, axial separations, and associated boundary



Table I Run Description

Design Run Identification Letter	Title	Aperture Ratio		Axial Focal Length (in.)	First Element Diameter (in.)	Entrance Pupil Diameter (in.)	Spectral Range (nm)	Field-of-View (deg)	Material
		Basic	With Relay						
A	33CD Original Foveal Lens Design	5.6	2.8	2	8	0.360	480-640	160	Glass F2 & SK16
B	08 Front Triplet Half Size	11	5.6	2	4	0.180	480-640	160	Glass F2 & SK16
C	108 Front Triplet Half Size	6	3	2	4	0.324	480-640	160	Glass F2 & SK16
D	108D Front Triplet Half Size 0.0675 Pupil	7.4	3.7	2	4	0.270	480-640	160	Glass F2 & SK16
E	13A Four in., Conf 50.8 Alternate Variables	12	6	2	2	0.162	480-640	160	Glass F2 & SK16
F	17 Front Triplet Half Size 0.59 to 0.85	6	3	2	4	0.324	588-852	160	Theoretical Glass
G	09 Double Gauss Relay	3	NA	2:1 Conjugates	NA	NA	480-640	160	Glass LAK N12, SK51, SSK4, SF7, F8
H	25 Front Triplet Half Size Spline Field Lens	6	3	2	4	0.324	480-640	NA	Glass F2, SK16, SF-15, LAK 3
I	23 Front Triplet Half Size IR Materials Change FOV = 60	6	3	2	4	0.324	588-852	120	Glass/Plastic SF19/Acrylic, SK16/Styrene
J	20 Front Triplet Half Size 0.59 to 0.94	6	3	2	4	0.324	588-852	160	F2, SK16, SF52
K	20A Front Triplet Half Size 0.59 to 0.94	6	3	2	4	0.324	588-940	160	F2, SK16, SF52
L(G+H)	25A Front Triplet Half Size with Relay	6	3	1	4	0.324	480-640	160	G + H

limits by the scale factor and multiplication of curvatures by the reciprocal of the scale factor. Only the front triplet portion of the foveal lens was rescaled. The triplet diameter is controlled by boundary limits, which are tied to the numerical aperture. The optimization program automatically scales input prescriptions to unit focal length. When scaling, the optimization program does not correctly compute the spline values. Therefore, to prevent automatic rescaling from occurring, the curvature of the surface preceeding the aperture stop was manually changed to bring the paraxial marginal ray through the stop at the same slope as in the original design thereby providing an input prescription, which has been manually set to unit focal length. The rescaled design was then optimized using damped least squares followed by an orthonormal optimization mode. The meridional ray intercepts of the new design, B, were then compared with A scaled to the same focal length on Figure 22. Note that blur diameters are essentially equal in either case. This is as predicted by the F/No., size, resolution parametrics of Figure 9 that were generated by geometrical optics extrapolations from our existing lens. That figure is repeated for convenience as Figure 23. The peak blurs from Figure 22 are also annotated on this figure. Note the agreement of Case B with theoretical curves. The parametrics of Figure 8 were further verified by running the lens optimization program first for a smaller F/number, while maintaining the same lens size (Run C), and then by reducing clear aperture, while maintaining F/number constant (Run E). Again, the peak blurs shown on Figure 23 were quite close to those predicted in Figure 23.

Data of Figures 22 and 23 plus the reasonable lens profiles of the best configurations shown in Figure 24 convinced us of the optimization program's validity. However, since practical considerations limit the foveal lens focal length to 2 inches (see Section 3), an optical relay is necessary to achieve correct image size. Before proceeding, we felt it best to determine the feasibility of such a relay.

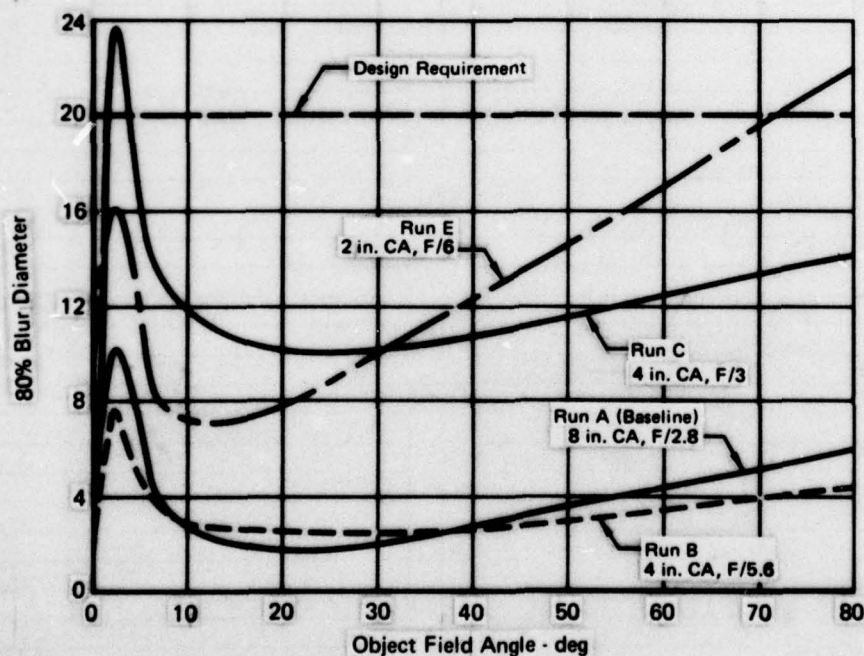


Figure 22 Visual Lens Performance - 1 In. Focal Length

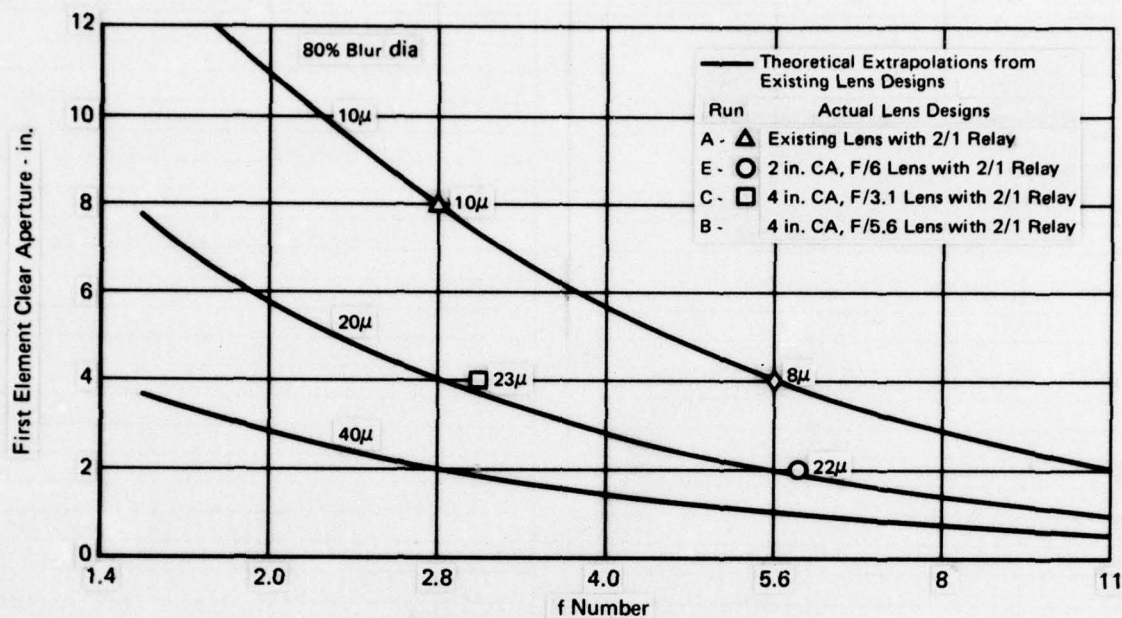


Figure 23 Theoretical Lens Size Parametrics  
Effective Focal Length = 1 In.

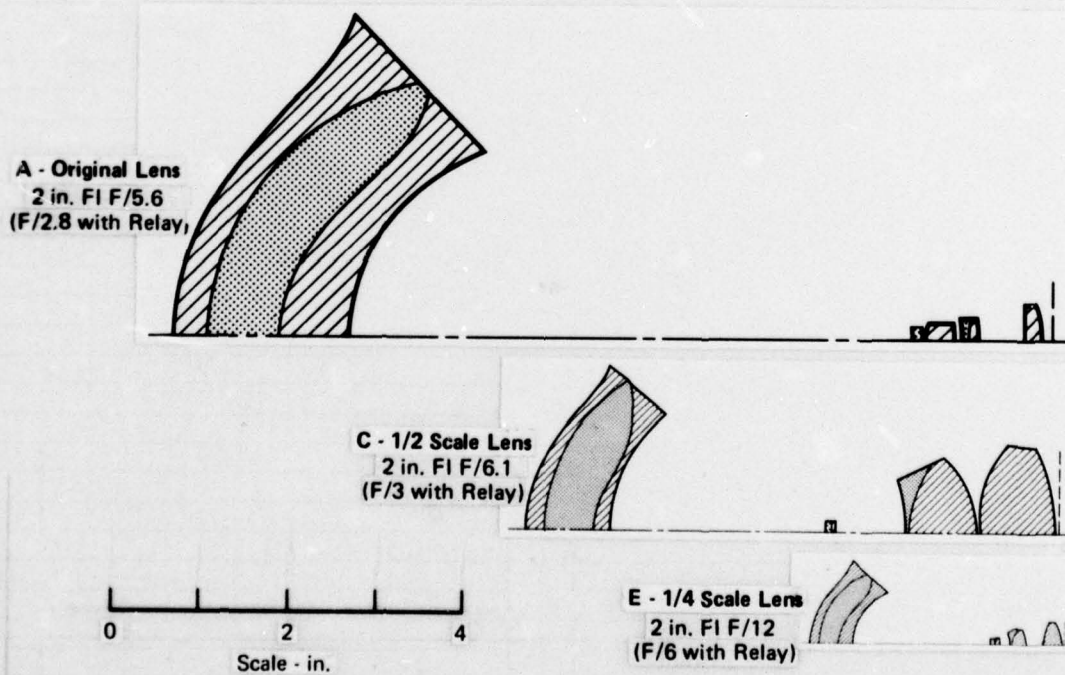


Figure 24 Visual Optical Designs



## B. OPTICAL RELAY CONFIGURATION

Using the C design as a starting point, a look at the chief rays exiting from the foveal lens indicated the presence of considerable shift of the exit pupil image with field angle. Figure 25A is a chief ray plot from C. A spline field lens eliminates this position shift and would then permit the design of a double Gauss relay, which can operate at system aperture ratios of F/3 (Figure 25B). One alternative to a spline field lens is to stay with a conventional relay lens configuration operating at a comparative aperture ratio of F/1, which requires the use of more lens elements to obtain the same degree of image quality (Figure 25C). Another alternative would be to use an external entrance pupil relay design with a comparative aperture ratio of F/3. This is not conventional and would require additional lens elements for aberration correction (Figure 25D).

After considering the predicted complexity of the various relay options, the spline field lens approach was selected as being the lowest cost with the greatest probability of providing satisfactory image quality in a minimum package size. Another consideration in selection of the spline field lens approach for further study was that the exit pupil formed by the field lens could be used as an aperture stop in the system more conveniently than the stop location inside the existing foveal lens design.

The spline field lens was manually configured to form a stationary exit pupil image for five off-axis field angles (2-1/2, 7-1/2, 20, 40, and 80 degrees). One spline segment was used for each angle making the field lens a five spline surface (the special surfaces in the foveal lens are defined by four splines each). After manually configuring the field lens, the foveal lens system, including the field lens, was optimized using the automatic design program resulting in design H. Performance of this configuration is shown on Figure 26. In parallel with this portion of the study, a double Gauss relay was optimized, G, at 2:1 conjugates using the image size of the foveal lens as an object and using the foveal lens exit pupil location as an object distance for the relay. The optimized relay was then added to H and performance of the resultant system, L, was computed. The performance of this combined system is also shown on Figure 26. It is clear from these data that the relay is contributing excessive degradation to image quality. It was clear from blur plots that the relay had excessive flare, i.e., the extreme marginal rays were diverging excessively. For this reason, a stop was placed in the relay to limit energy transfer to the center 50% of the ray bundles. These data, also plotted on Figure 26, show very good performance. In fact, it suggests more of the ray bundle could be utilized effectively, while still meeting design requirements.

In conclusion, the above results indicate the spline field lens is performing properly. In addition, the relay optical flare noted above is a well-known characteristic of the double Gauss design, and correction of this problem is covered by many sources, e.g., Reference 4. For these reasons, we decided to

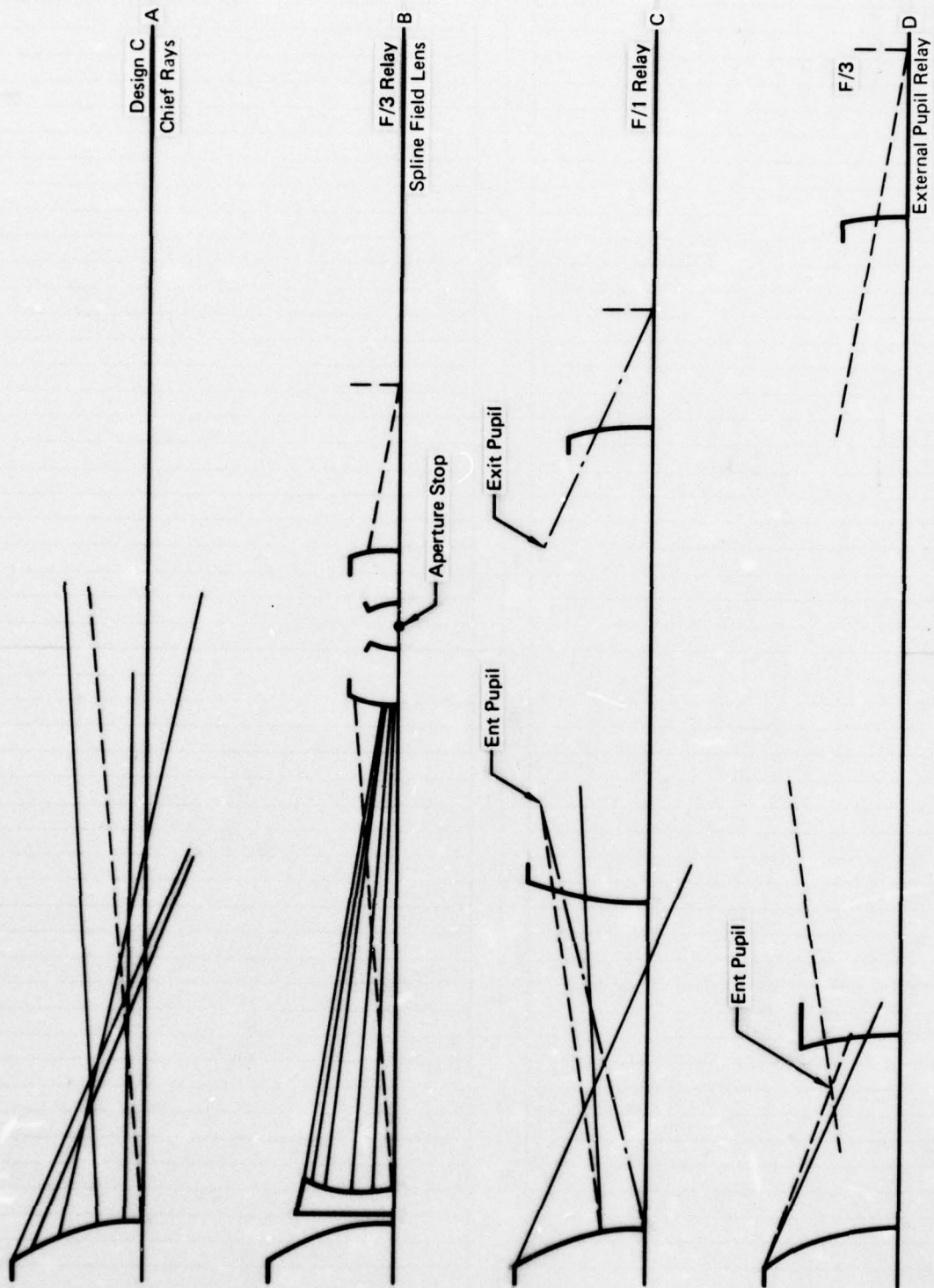


Figure 25 Optical Relay Considerations

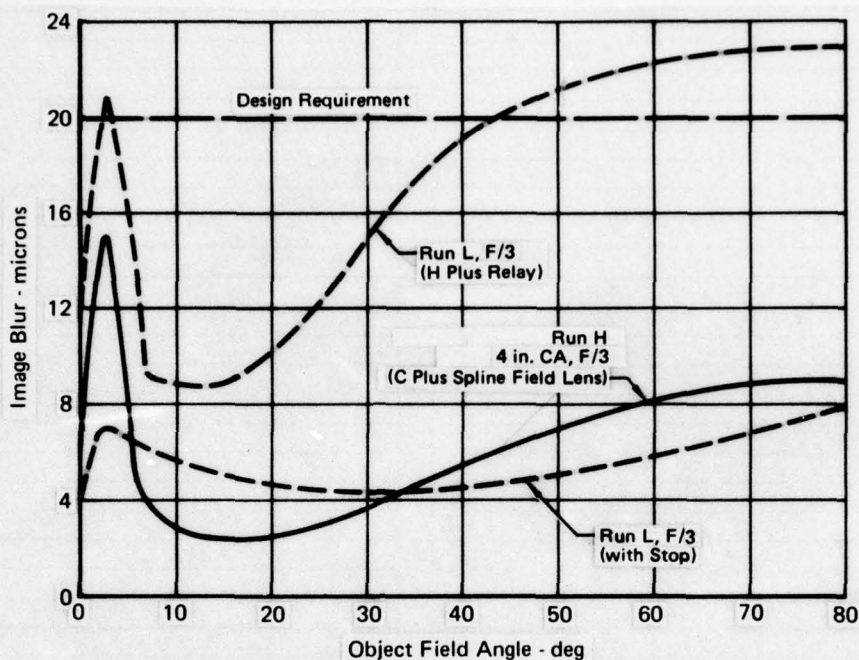


Figure 26 Optical Relay Performance

terminate work on the relay and concentrate on design and optimization of the basic lens. For reference, the L lens, which terminates this effort, is shown in Figure 27.

### C. EXTENSION OF SPECTRAL RESPONSE

For an analysis of spectral shift to longer wavelengths on the system performance, configuration C was taken as a starting point, and the refractive index and dispersion values for the prescription were changed to correspond to the region 588 nm to 852 nm using a mean wavelength of 687 nm. Because the mean for the visible was at 546 nm, the optimization program rescaled the focal length shift and corresponding manual changes to the splines were required. Having completed the prescription setup, the design program was utilized to optimize the resolution performance for this shifted spectral region using refractive index and dispersion of the lens elements in addition to the previously used variables. After optimizing, this configuration was designated Run F. Its performance is shown on Figure 28. The results were very encouraging - performance was better than Run C on Figure 22. Some improvement was expected from the behavior of refractive index in this spectral range compared to the visual spectral range.

It should be noted that a glass materials optical performance math model was used by the computer for this optimization; i.e., the computer uses a continuous index/dispersion function that is representative of available glasses. During the materials study and final optimization phase, actual glass types are substituted that most closely match computer selected parameters.



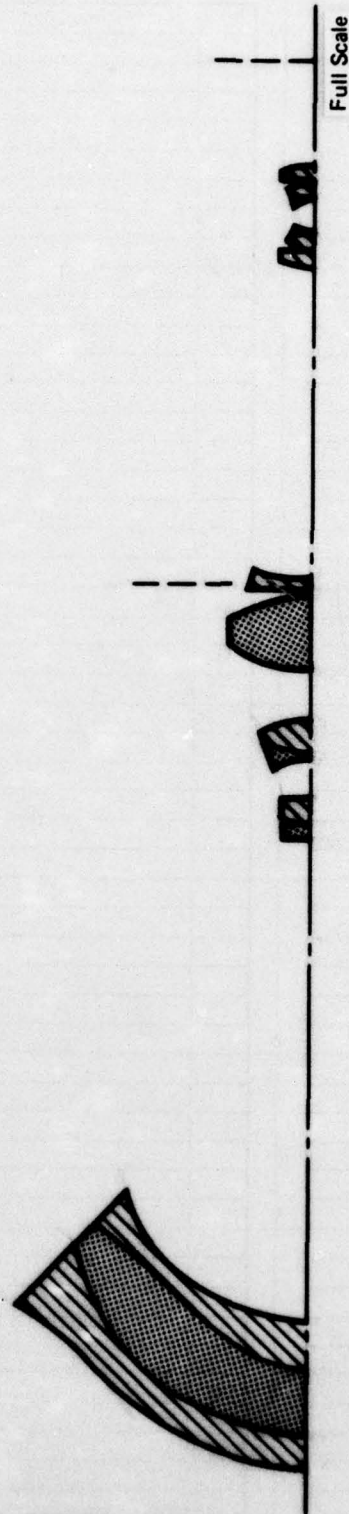
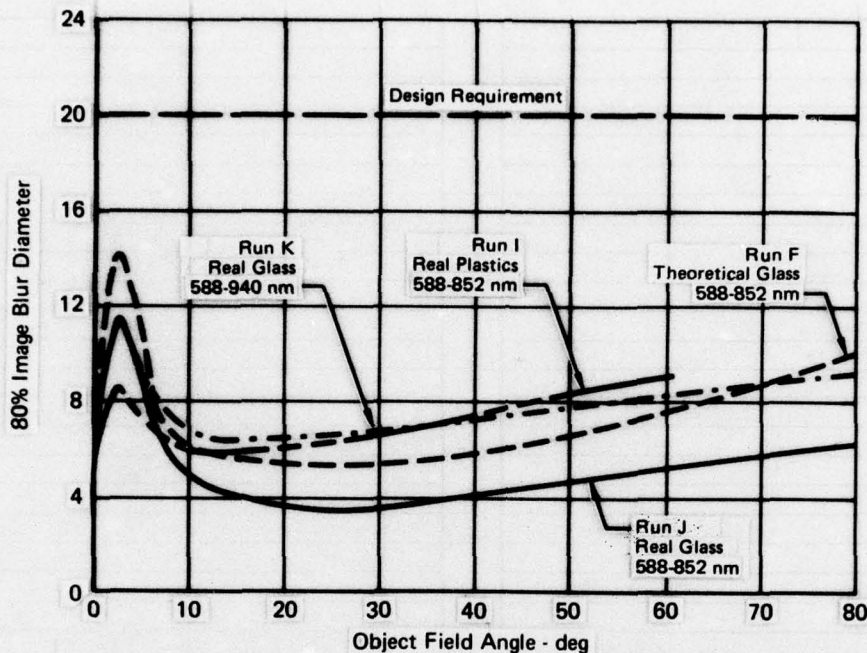


Figure 27 Configuration L Optical Design  
1 In. Focal Length  $F/3$



**Figure 28 Extended Spectral Range Configurations**  
1 In. Effective Focal Length, F/3, 4 In. Clear Aperture

#### D. MATERIALS STUDY AND FINAL OPTIMIZATION

The optimized glass IR design using theoretical glass, F, was used as a starting point for evaluation of the possibility of fabricating the spline lens elements from plastics. The mapping function for the foveal lens is primarily achieved at the first lens surface. In the glass design this surface is a spline and required a refractive index of 1.62 with an incidence angle of approximately 70° in order to obtain the required bending of the edge field chief ray. Bending of the chief rays along the same path with a representative plastic material of index 1.49 would require even steeper incidence angles, which is analogous to asking for more work from the first spline surface. A reduction of the sine of the incidence angle in proportion to the refractive index change in going from glass to plastic will keep the work load on the first surface constant, thereby making performance comparisons with the preceeding designs more valid. The change in incidence angle amounts to reducing the field of view to 120°. The result of optimizing the foveal lens with acrylic and styrene materials on the spline elements is shown as I on Figure 28. Surprisingly, performance is better than run F, the glass design. Some of this improvement (about 5%) would be expected due to effective distortion reduction caused by the smaller FOV. The remainder of this improvement may be due to a higher degree of optimization being achieved through repeated iterations and the resulting higher level of familiarity with the 4 inch clear aperture, F/3 lens configuration. This can also be seen in Run J, which is the result of replacing the theoretical glass parameters of Run F with real glass parameters for repeated computer optimization runs. Again, performance exceeds Run F, indicating a greater degree of optimization. The lens configurations of Runs I and J are shown in Figure 29.

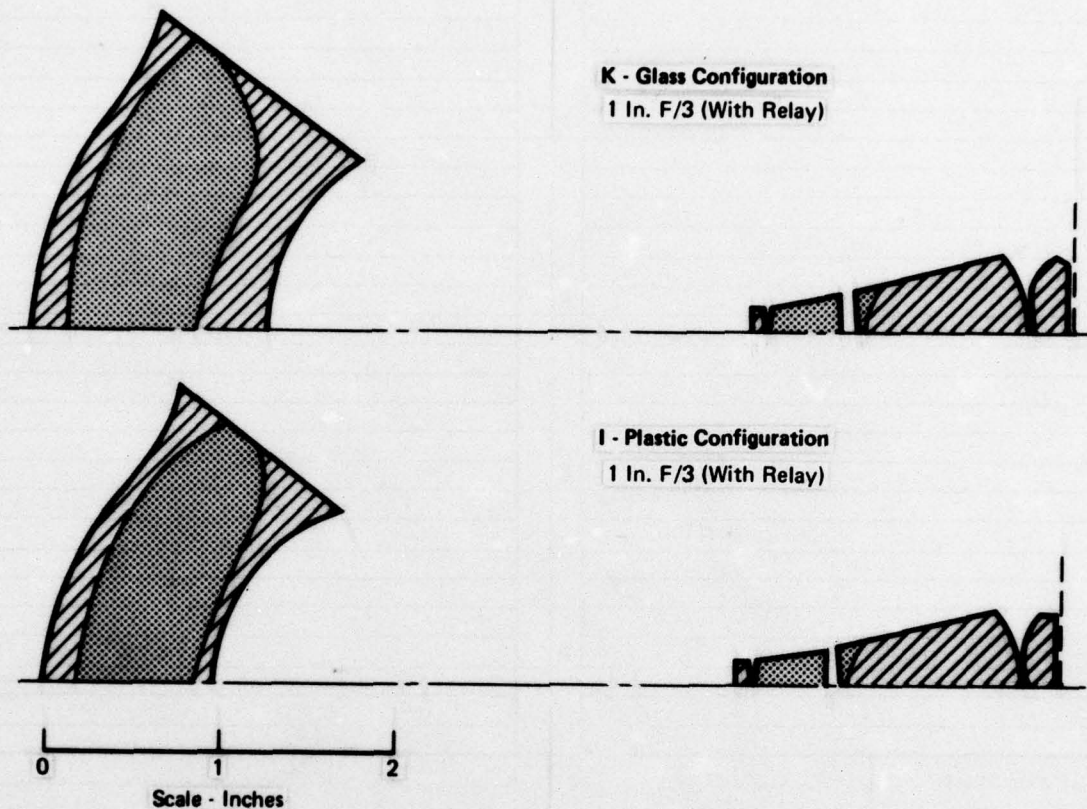


**Figure 29 Optical Designs - Extended Spectrum**

As a final step in the study, Configuration J was evaluated over the spectral range of 588-940 nm, which covers most of the sensitivity range of the proposed silicon CCD sensing array. This performance is shown as K on Figure 28. Note performance is only slightly degraded from Run J. However, performance is still twice as good as the original design specification of  $20\mu$ .



## Section VI

### CONCLUSIONS AND RECOMMENDATIONS

#### A. CONCLUSIONS

In general, results were more favorable than expected. The final optimized miniature lens design, I (plastic) and K (glass), performed approximately two times better than expected. This, in itself, raises two valid questions, which are:

- o Why did the lens exceed performance estimates?
- o Could the lens be made still smaller?

To examine the first question, we carefully reviewed all computer runs. A key, we believe, can be seen in Table 1. All sample configurations that agreed with our geometrical optics extrapolations from our existing lens A utilized only F/2 and SK-16 glass types. This was found to be a constraint on all these design runs. When it was removed (after case E), the performance steadily improved. This leads one to the conclusion that, very possibly, our original lens A was not completely optimized. We are presently rerunning this lens without the "glass type" constraint. While results are not available at this writing, we will continue this investigation to resolve this apparent inconsistency.

If it is true that twice the optical quality can be achieved from any foveal lens than originally anticipated, the geometrical optical predictions of Figure 9 must be revised as shown in Figure 30. Based on these curves, a 1/4 scale lens of the same F/number is feasible that still meets our original specifications. Such a lens would be similar to configuration E of Figure 24. With its relay, this lens could be packaged as shown in Figure 31. When it is compared to possible packaging of configuration K, the advantage of further miniaturization is seen to be approximately a 40% reduction in length, about 30% reduction in height, and a 50% reduction in width. Weight would be approximately 1/2 that of the larger lens.

We believe there is a very valid technical reason for staying with the larger, higher performance lens. This lies in its ability to support a higher resolution CCD or optical image magnification. Since the latter is the most stringent requirement, it was studied in detail using the systems model developed in Section 4.

Magnification is included in this model by simply changing all S values to the right of the lens/optical MTF to S/M. Results were obtained for magnifications of 2 and 4 and lens qualities ( $\tau_1$ ) representing 10 $\mu$  and 20 $\mu$  image blur values. These results are shown on Figure 32. Note that changing from a 10 $\mu$  to 20 $\mu$  lens quality has almost no effect at unity magnification (percentage wise); while at 2x, it lowers low contrast performance between 10 and 20%. At 4x magnifications of this degradation increase to the 30 to 40% range. The 10 $\mu$  lens can easily support 4x magnification, while the 20 $\mu$  lens cannot.

Added to the above concerns with the 1/4 scale lens is that of fabrication feasibility. There may be considerable technical risk in achieving the high surface slopes required for the small lens, while maintaining adequate tolerances. This, we believe, is pushing state-of-the-art in aspheric fabrication for either glass or plastics.

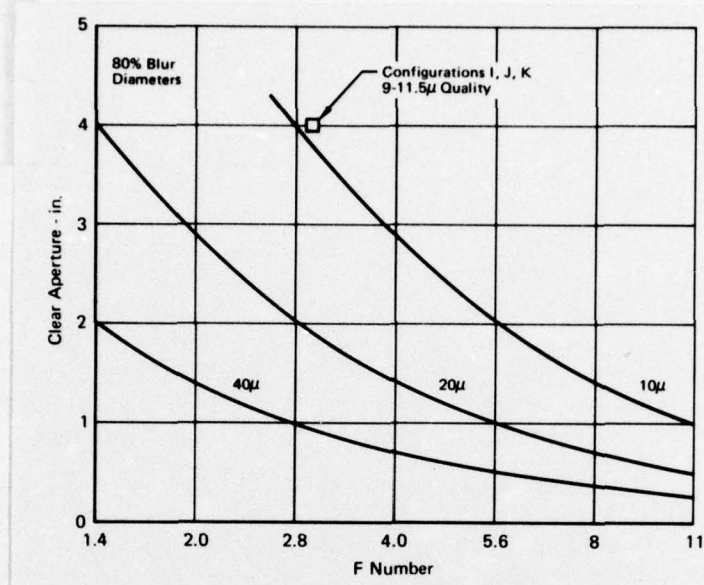


Figure 30 Revised Foveal Lens Size Parametrics

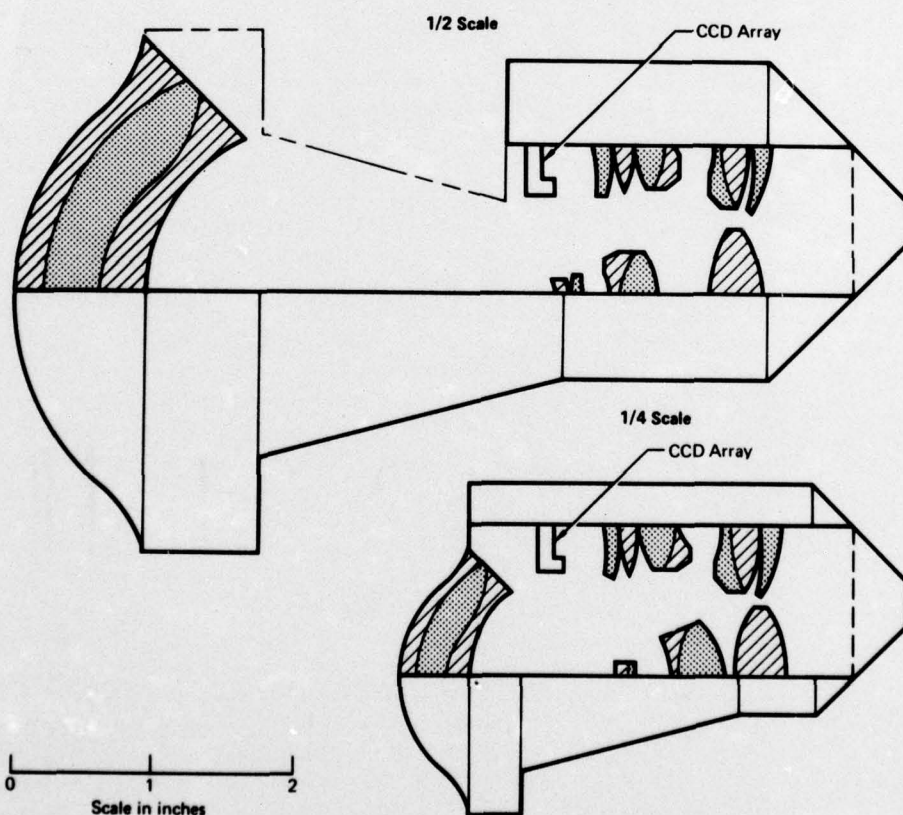
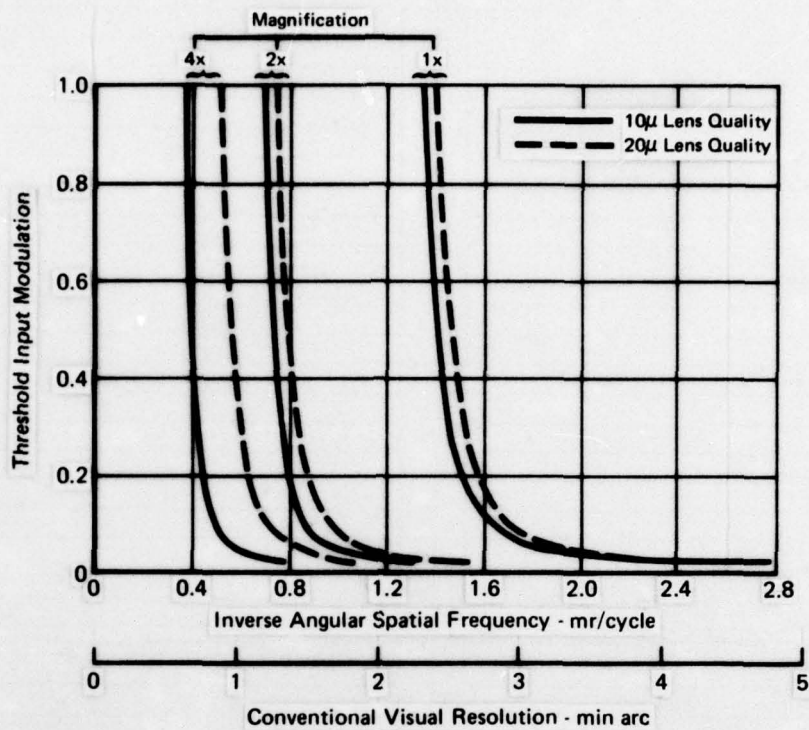


Figure 31 Possible Lens Layouts



**Figure 32 Minimum Resolvable Contrast with Image Magnification**  
1 In. Focal Length Lens Plus RCA SID 51232 - 100 fL Display

## B. RECOMMENDATIONS

Based on concerns listed above, we recommend a half-scale lens similar to that of optical designs K or I be fabricated. We believe either is well within the state-of-the-art; however, the facts are:

- o Only 120° FOV has been theoretically proven for the plastic lens compared to 160° for the glass configuration.
- o Thermal problems are known to exist with the plastic lens (see Section 3). Mechanical compensation would positively be required. This would involve considerable non-recurring costs to assure maximum optical performance, mechanical rigidity, and good service life.

At this point it appears that the best approach would be to fabricate a lens of the plastic design, I, but use glass with optical characteristics identical to the plastics. This design could be prototyped and tested inexpensively. Later, as production requirements and quantities become firm, it could be converted to plastics to reduce costs.



## Appendix

### SAMPLE LENS DESIGN COMPUTER RUN

The following pages contain a sample lens design computer run. Approximately 100 runs were required and were analyzed in order to finalize the lens prescription.

SEE UPDATE 18/ 1/71

NAME: RAD SASC, MNA

1-10

1-10

1-10

1-10

1-10

1-10

1-10

1-10

1-10

1-10

1-10

1-10

1-10

1-10

1-10

1-10

1-10

1-10

1-10

1-10

1-10

1-10

1-10

1-10

1-10

1-10

1-10

1-10

1-10

1-10

1-10

1-10

1-10

1-10

1-10

1-10

1-10

1-10

1-10

1-10

1-10

1-10

1-10

1-10

1-10

1-10

1-10

1-10

1-10

1-10

1-10

1-10

1-10

1-10

1-10

1-10

1-10

1-10

1-10

1-10

1-10

1-10

1-10

















5030

[illegible]

9926-89

[illegible]

A 4x4 grid of 16 small images. Each image shows a different combination of the letters 'N', 'U', and 'M' in various orientations and positions, illustrating the concept of a 4x4 matrix.

[illegible]

Account	2019	2018	2017	2016	2015	2014	2013	2012	2011	2010	2009	2008	2007	2006	2005	2004	2003	2002	2001	2000	1999	1998	1997	1996	1995	1994	1993	1992	1991	1990	1989	1988	1987	1986	1985	1984	1983	1982	1981	1980	1979	1978	1977	1976	1975	1974	1973	1972	1971	1970	1969	1968	1967	1966	1965	1964	1963	1962	1961	1960	1959	1958	1957	1956	1955	1954	1953	1952	1951	1950	1949	1948	1947	1946	1945	1944	1943	1942	1941	1940	1939	1938	1937	1936	1935	1934	1933	1932	1931	1930	1929	1928	1927	1926	1925	1924	1923	1922	1921	1920	1919	1918	1917	1916	1915	1914	1913	1912	1911	1910	1909	1908	1907	1906	1905	1904	1903	1902	1901	1900	1899	1898	1897	1896	1895	1894	1893	1892	1891	1890	1889	1888	1887	1886	1885	1884	1883	1882	1881	1880	1879	1878	1877	1876	1875	1874	1873	1872	1871	1870	1869	1868	1867	1866	1865	1864	1863	1862	1861	1860	1859	1858	1857	1856	1855	1854	1853	1852	1851	1850	1849	1848	1847	1846	1845	1844	1843	1842	1841	1840	1839	1838	1837	1836	1835	1834	1833	1832	1831	1830	1829	1828	1827	1826	1825	1824	1823	1822	1821	1820	1819	1818	1817	1816	1815	1814	1813	1812	1811	1810	1809	1808	1807	1806	1805	1804	1803	1802	1801	1800	1799	1798	1797	1796	1795	1794	1793	1792	1791	1790	1789	1788	1787	1786	1785	1784	1783	1782	1781	1780	1779	1778	1777	1776	1775	1774	1773	1772	1771	1770	1769	1768	1767	1766	1765	1764	1763	1762	1761	1760	1759	1758	1757	1756	1755	1754	1753	1752	1751	1750	1749	1748	1747	1746	1745	1744	1743	1742	1741	1740	1739	1738	1737	1736	1735	1734	1733	1732	1731	1730	1729	1728	1727	1726	1725	1724	1723	1722	1721	1720	1719	1718	1717	1716	1715	1714	1713	1712	1711	1710	1709	1708	1707	1706	1705	1704	1703	1702	1701	1700	1699	1698	1697	1696	1695	1694	1693	1692	1691	1690	1689	1688	1687	1686	1685	1684	1683	1682	1681	1680	1679	1678	1677	1676	1675	1674	1673	1672	1671	1670	1669	1668	1667	1666	1665	1664	1663	1662	1661	1660	1659	1658	1657	1656	1655	1654	1653	1652	1651	1650	1649	1648	1647	1646	1645	1644	1643	1642	1641	1640	1639	1638	1637	1636	1635	1634	1633	1632	1631	1630	1629	1628	1627	1626	1625	1624	1623	1622	1621	1620	1619	1618	1617	1616	1615	1614	1613	1612</
---------	------	------	------	------	------	------	------	------	------	------	------	------	------	------	------	------	------	------	------	------	------	------	------	------	------	------	------	------	------	------	------	------	------	------	------	------	------	------	------	------	------	------	------	------	------	------	------	------	------	------	------	------	------	------	------	------	------	------	------	------	------	------	------	------	------	------	------	------	------	------	------	------	------	------	------	------	------	------	------	------	------	------	------	------	------	------	------	------	------	------	------	------	------	------	------	------	------	------	------	------	------	------	------	------	------	------	------	------	------	------	------	------	------	------	------	------	------	------	------	------	------	------	------	------	------	------	------	------	------	------	------	------	------	------	------	------	------	------	------	------	------	------	------	------	------	------	------	------	------	------	------	------	------	------	------	------	------	------	------	------	------	------	------	------	------	------	------	------	------	------	------	------	------	------	------	------	------	------	------	------	------	------	------	------	------	------	------	------	------	------	------	------	------	------	------	------	------	------	------	------	------	------	------	------	------	------	------	------	------	------	------	------	------	------	------	------	------	------	------	------	------	------	------	------	------	------	------	------	------	------	------	------	------	------	------	------	------	------	------	------	------	------	------	------	------	------	------	------	------	------	------	------	------	------	------	------	------	------	------	------	------	------	------	------	------	------	------	------	------	------	------	------	------	------	------	------	------	------	------	------	------	------	------	------	------	------	------	------	------	------	------	------	------	------	------	------	------	------	------	------	------	------	------	------	------	------	------	------	------	------	------	------	------	------	------	------	------	------	------	------	------	------	------	------	------	------	------	------	------	------	------	------	------	------	------	------	------	------	------	------	------	------	------	------	------	------	------	------	------	------	------	------	------	------	------	------	------	------	------	------	------	------	------	------	------	------	------	------	------	------	------	------	------	------	------	------	------	------	------	------	------	------	------	------	------	------	------	------	------	------	------	------	------	------	------	------	------	------	------	------	------	------	------	------	------	------	------	--------



**6 2 7 2 8**

11-2117  
515







```

06087777 -1796558 2103.506
COLOR LONGE -1796558 2103.506
TOTAL LENGTH= 4.9997 34
          .30032827 -16.176249
          .100990 .027922

```

















DOLD=	2.883195-10	1.213947E-06	MRM	NLM	MRED	RMSE	Q1+2	Q2+2	VCS+2	CHNG+2	RED+2
26	0	1	9	0	-6	5	389	70	0	99	0
RAY 6 SURFACE 2CF	1	1	9	0	-6	5	389	70	0	99	0
30	0	1	7	0	0	3	1081	74	0	99	0
RAY 6 SURFACE 2CF	1	1	7	0	0	3	1081	74	0	99	0



115 113 111 109 107 105 103 101 99 97 95 93 91 89 87 85 83 81 79 77 75 73 71 69 67 65 63 61 59 57 55 53 51 49 47 45 43 41 39 37 35 33 31 29 27 25 23 21 19 17 15 13 11 9 7 5 3 1

2025-01-20 10:10:10

COLOR LO







DOL	2 =	0.062367E-10	
2	4.70	39282	24685
3	4.0385	37750	18769
4	3.562	3008	5766
5	38264	51968	71727
6	-000440	05239	10501
7	0.000000	05081	04347
8	-000471	05731	3169
9	-000515	05399	04763
10	-71027	07783	10000
11	-000000	12000	02332
12	-00341	12201	14664
13	-02749	12560	14767
14	-04087	22854	19763
15	-07090	23130	08044

5  
5  
5  
  
5  
5  
5  
5  
5  
5  
1  
5  
5

5  
5  
1  
1  
5  
5  
6  
2  
5  
1  
2  
2  
3  
3  
2



15	5.580000	-4.098000	4.734654	3028046	-4.4790706	4.067961	-2.321553
TOTAL LENGTH=1.489920							
B							
C							
D							
E							
F							
G							
H							
I							
J							
K							
L							
M							
N							
O							
P							
Q							
R							
S							
T							
U							
V							
W							
X							
Y							
Z							





1-19	0.	-0.63007700	-0.	1.00000000	0.	0.00000000	0.	.02700479	0.
2-19	1.	0.52505100E-01	1.	0.913030E-01	0.	0.1915130E-01	0.	0.39090000E-01	-1.49007417E+00
3-19	1.	0.01000000E-01	1.	0.00000000E-01	0.	0.00000000E-01	0.	0.00000000E-01	0.
4-19	1.	0.01000000E-01	1.	0.00000000E-01	0.	0.00000000E-01	0.	0.00000000E-01	0.
5-19	1.	0.01000000E-01	1.	0.00000000E-01	0.	0.00000000E-01	0.	0.00000000E-01	0.
6-19	1.	0.01000000E-01	1.	0.00000000E-01	0.	0.00000000E-01	0.	0.00000000E-01	0.
7-19	1.	0.01000000E-01	1.	0.00000000E-01	0.	0.00000000E-01	0.	0.00000000E-01	0.
8-19	1.	0.01000000E-01	1.	0.00000000E-01	0.	0.00000000E-01	0.	0.00000000E-01	0.
9-19	1.	0.01000000E-01	1.	0.00000000E-01	0.	0.00000000E-01	0.	0.00000000E-01	0.
10-19	1.	0.01000000E-01	1.	0.00000000E-01	0.	0.00000000E-01	0.	0.00000000E-01	0.
11-19	1.	0.01000000E-01	1.	0.00000000E-01	0.	0.00000000E-01	0.	0.00000000E-01	0.
12-19	1.	0.01000000E-01	1.	0.00000000E-01	0.	0.00000000E-01	0.	0.00000000E-01	0.
13-19	1.	0.01000000E-01	1.	0.00000000E-01	0.	0.00000000E-01	0.	0.00000000E-01	0.
14-19	1.	0.01000000E-01	1.	0.00000000E-01	0.	0.00000000E-01	0.	0.00000000E-01	0.
15-19	1.	0.01000000E-01	1.	0.00000000E-01	0.	0.00000000E-01	0.	0.00000000E-01	0.
16-19	1.	0.01000000E-01	1.	0.00000000E-01	0.	0.00000000E-01	0.	0.00000000E-01	0.

17-19	1.	-1.41779370E-02	-0.	0.00000000E-01	0.	0.00000000E-01	0.	0.00000000E-01	0.
-------	----	-----------------	-----	----------------	----	----------------	----	----------------	----

EFL,FP,PP2 1.00000 3.70317 -.00455



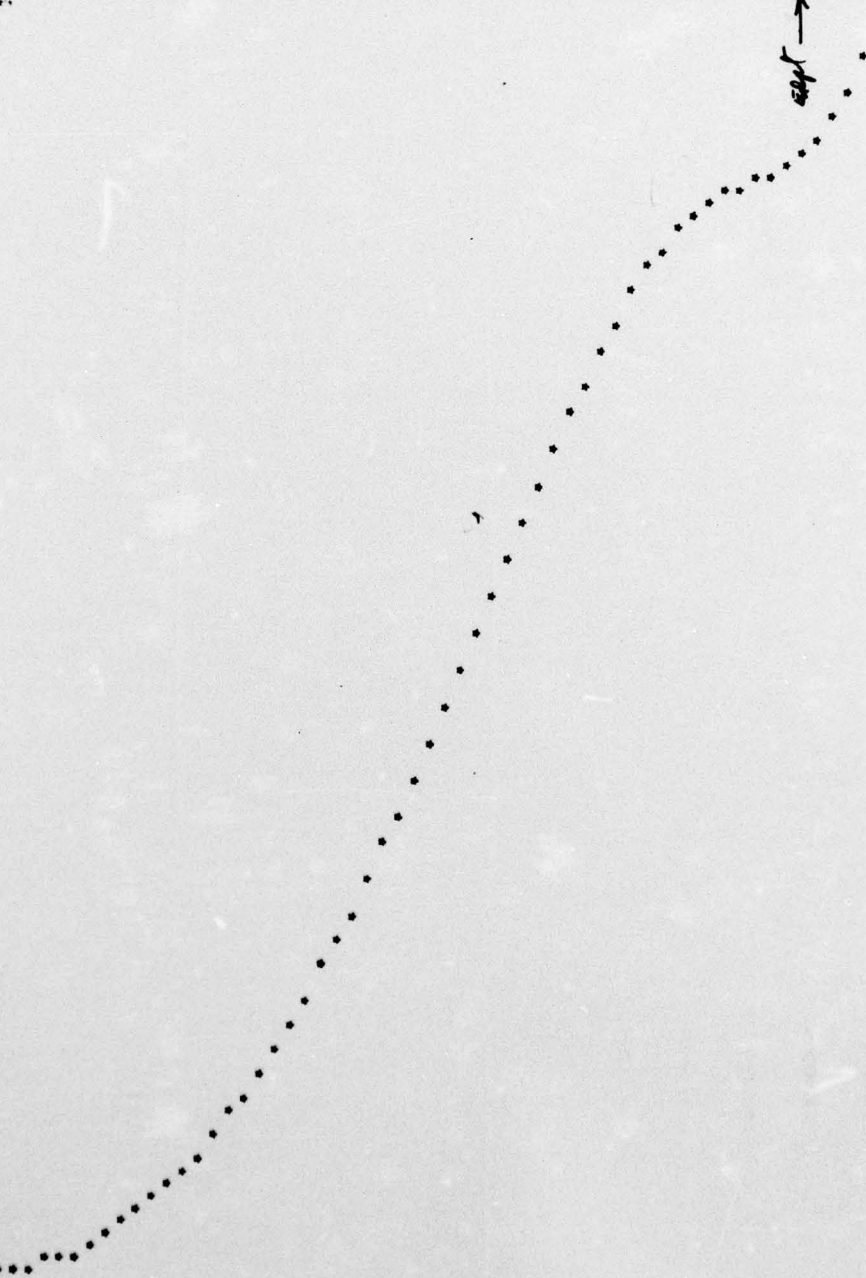


.....

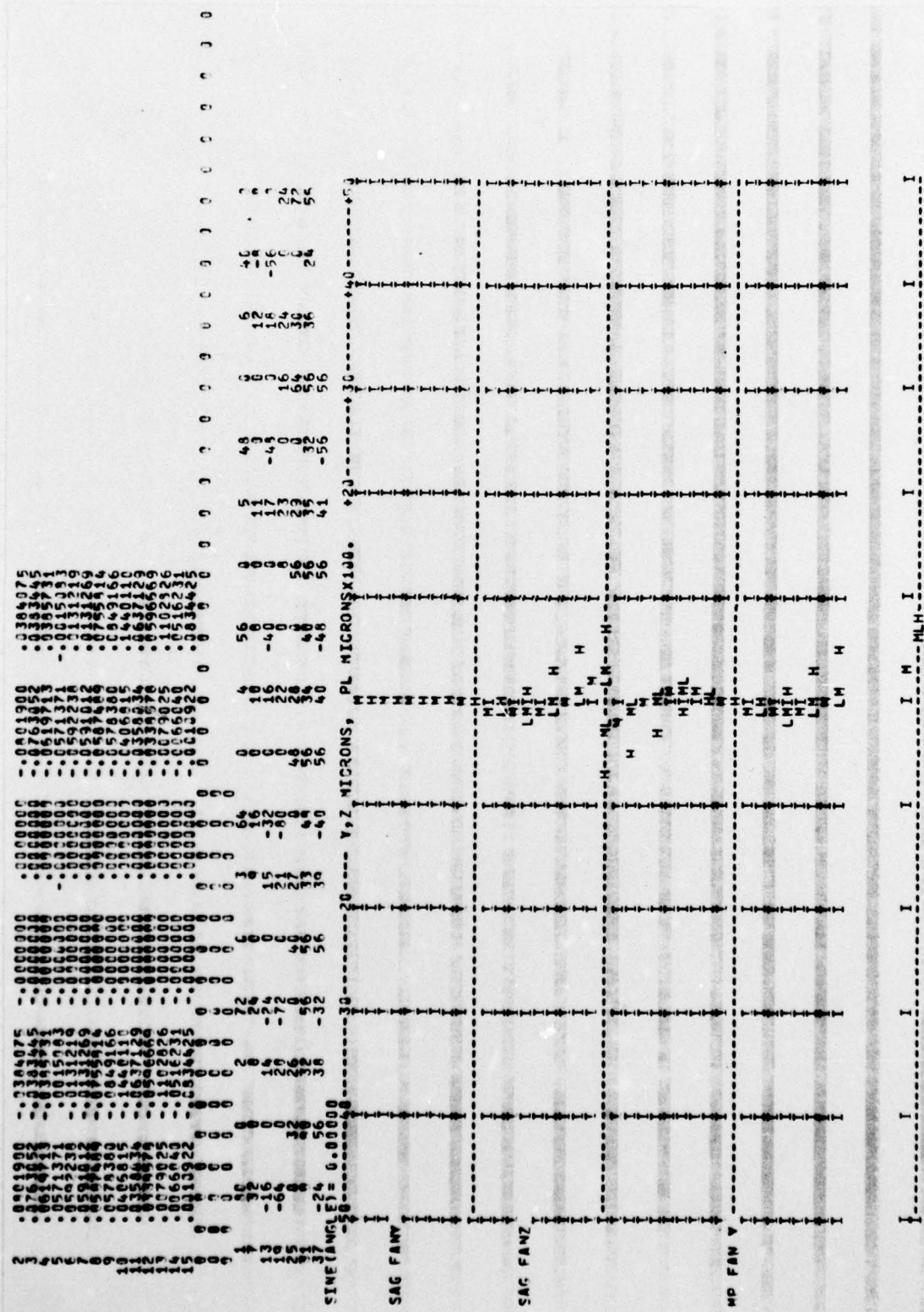
.....

.....

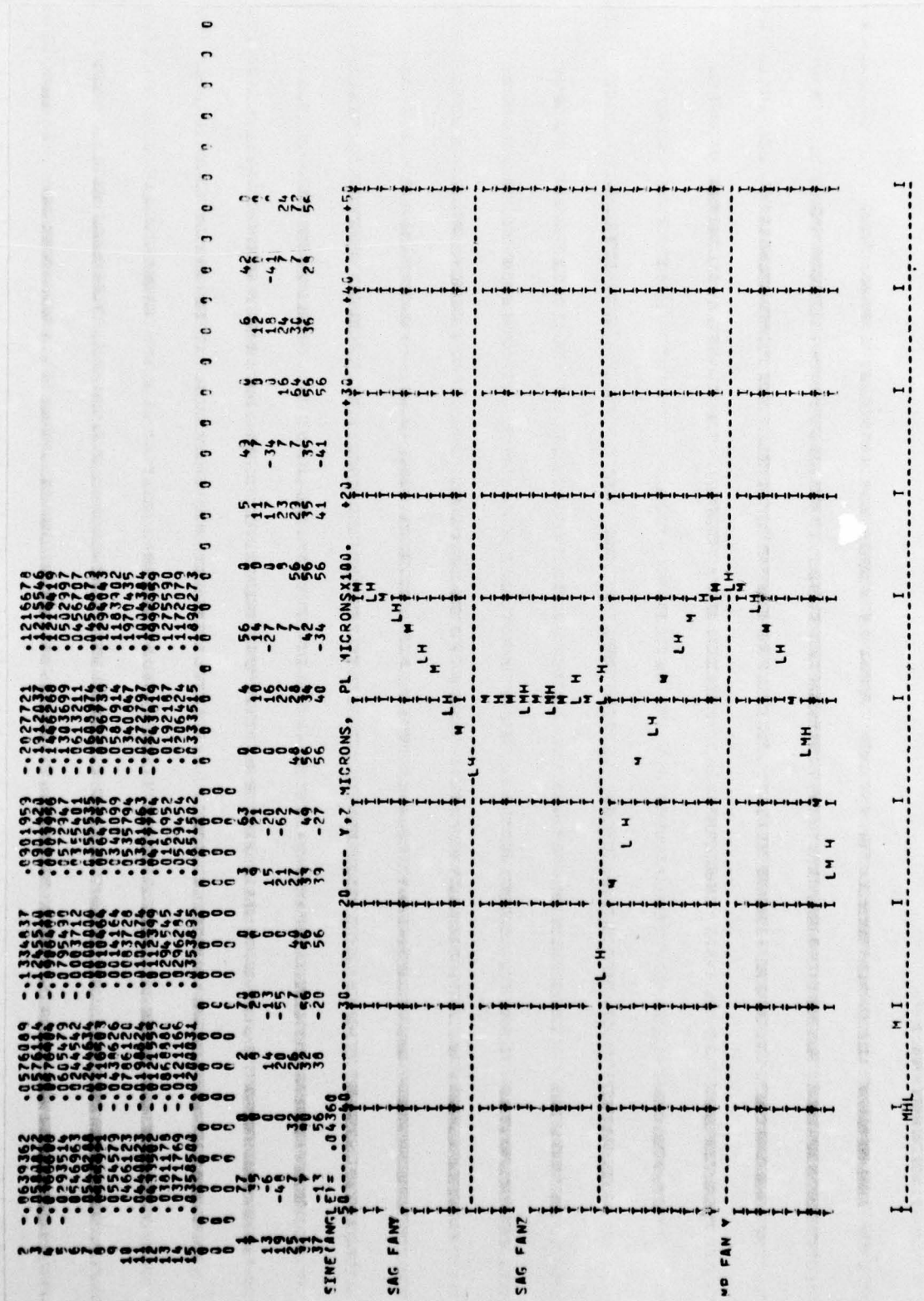
SURFACE \* ONE SPACE EQUALS \* 11355122

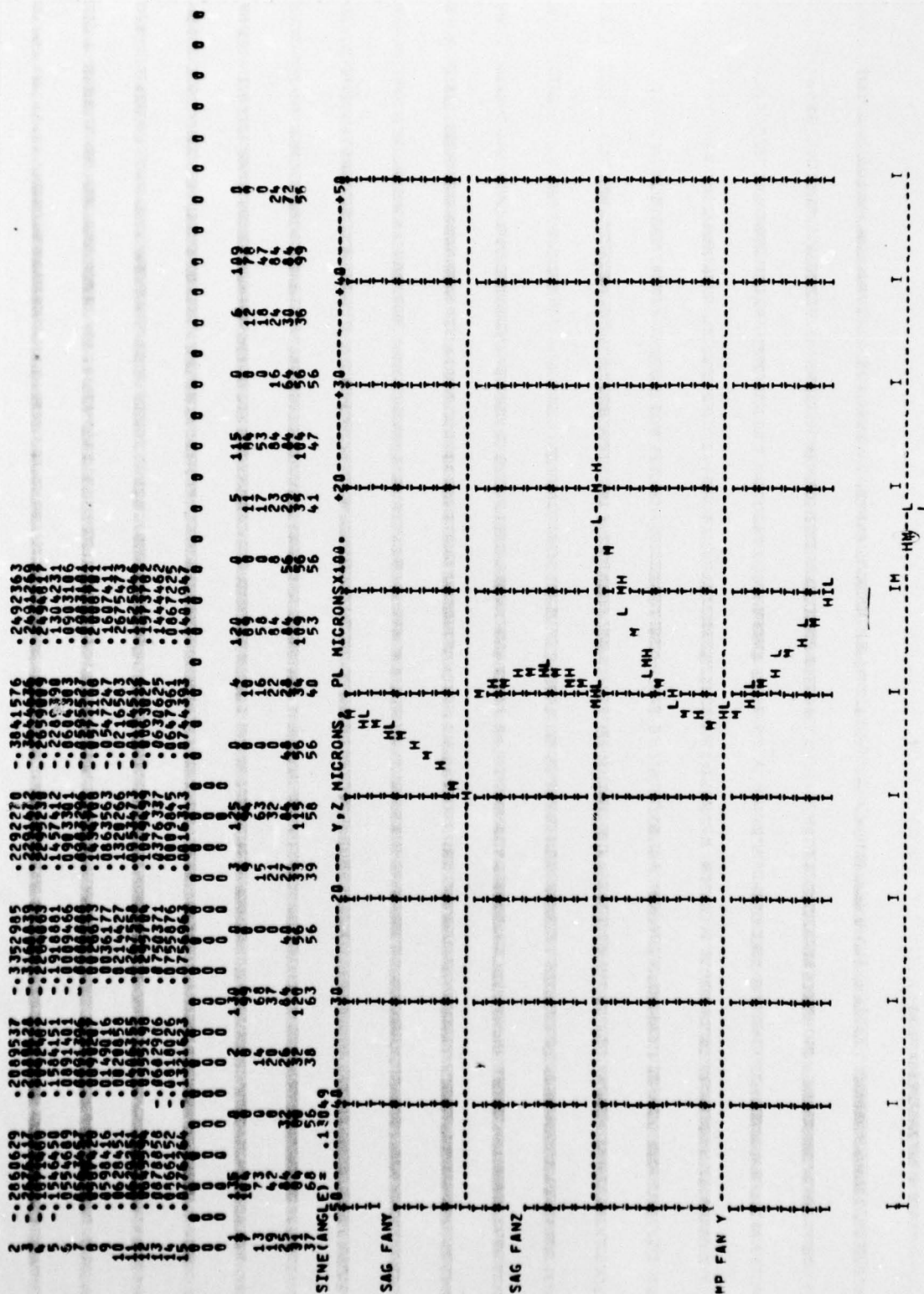


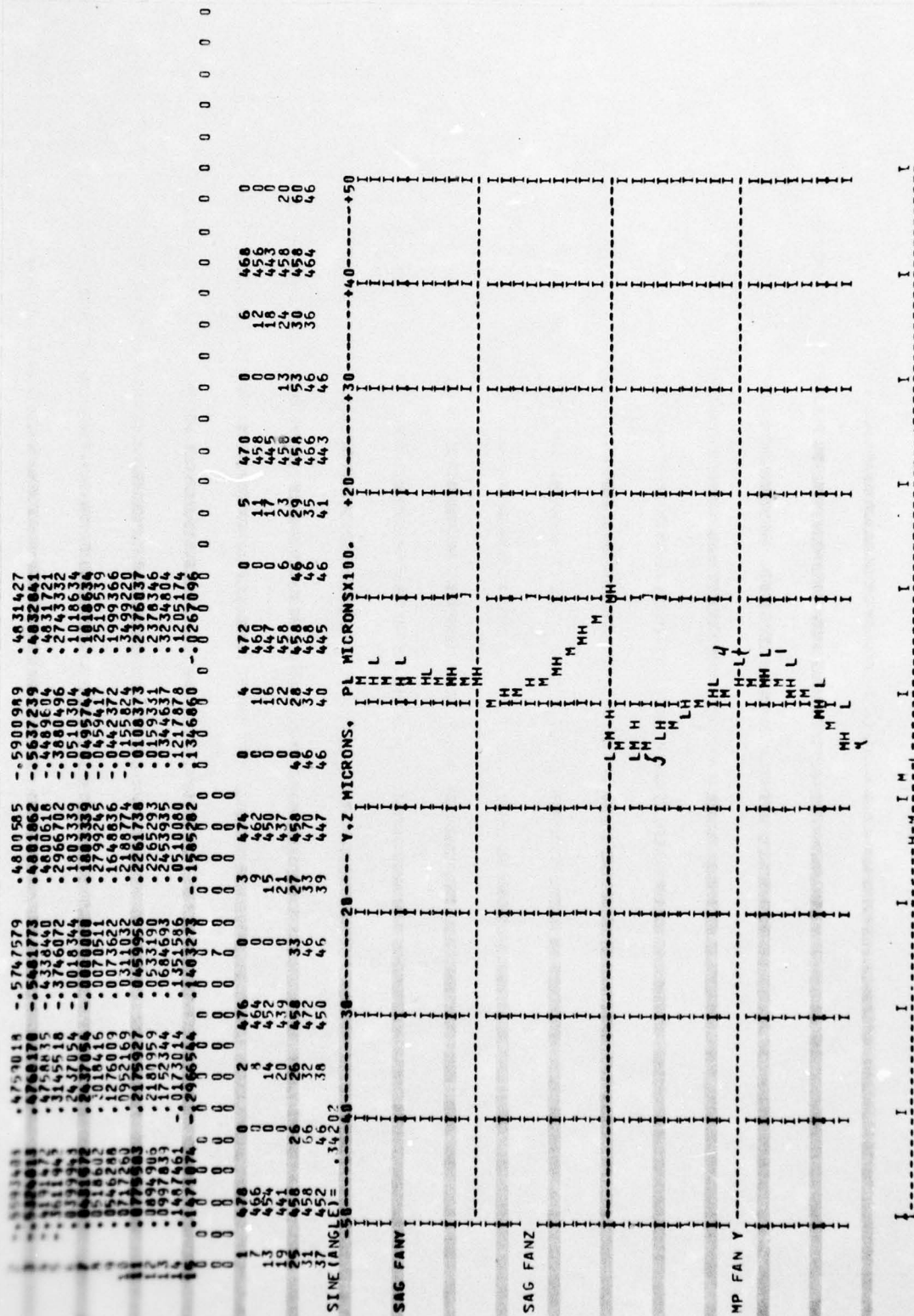




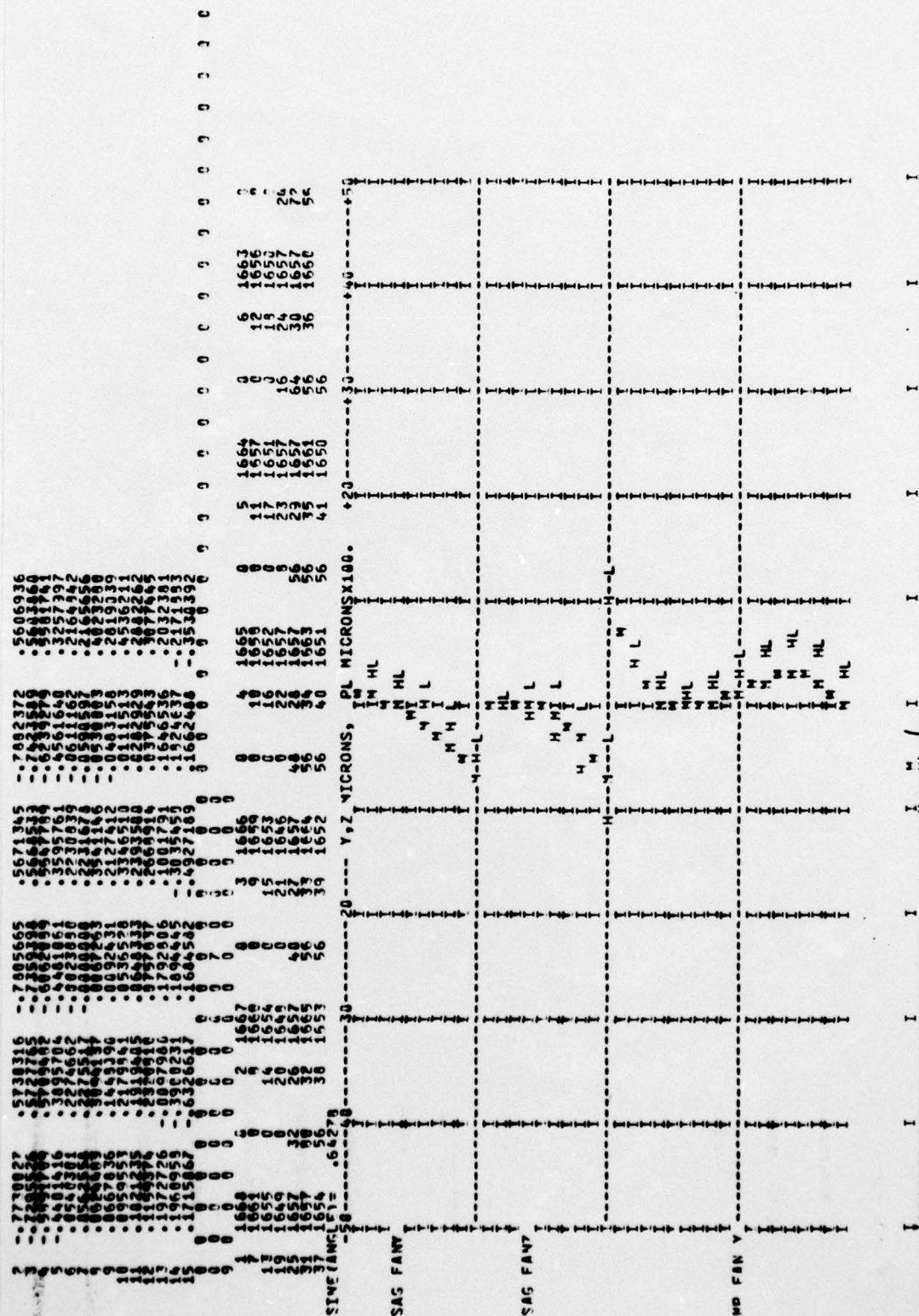




















317582  
 317581  
 317580  
 317579  
 317578  
 317577  
 317576  
 317575  
 317574  
 317573  
 317572  
 317571  
 317570  
 317569  
 317568  
 317567  
 317566  
 317565  
 317564  
 317563  
 317562  
 317561  
 317560  
 317559  
 317558  
 317557  
 317556  
 317555  
 317554  
 317553  
 317552  
 317551  
 317550  
 317549  
 317548  
 317547  
 317546  
 317545  
 317544  
 317543  
 317542  
 317541  
 317540  
 317539  
 317538  
 317537  
 317536  
 317535  
 317534  
 317533  
 317532  
 317531  
 317530  
 317529  
 317528  
 317527  
 317526  
 317525  
 317524  
 317523  
 317522  
 317521  
 317520  
 317519  
 317518  
 317517  
 317516  
 317515  
 317514  
 317513  
 317512  
 317511  
 317510  
 317509  
 317508  
 317507  
 317506  
 317505  
 317504  
 317503  
 317502  
 317501  
 317500  
 317499  
 317498  
 317497  
 317496  
 317495  
 317494  
 317493  
 317492  
 317491  
 317490  
 317489  
 317488  
 317487  
 317486  
 317485  
 317484  
 317483  
 317482  
 317481  
 317480  
 317479  
 317478  
 317477  
 317476  
 317475  
 317474  
 317473  
 317472  
 317471  
 317470  
 317469  
 317468  
 317467  
 317466  
 317465  
 317464  
 317463  
 317462  
 317461  
 317460  
 317459  
 317458  
 317457  
 317456  
 317455  
 317454  
 317453  
 317452  
 317451  
 317450  
 317449  
 317448  
 317447  
 317446  
 317445  
 317444  
 317443  
 317442  
 317441  
 317440  
 317439  
 317438  
 317437  
 317436  
 317435  
 317434  
 317433  
 317432  
 317431  
 317430  
 317429  
 317428  
 317427  
 317426  
 317425  
 317424  
 317423  
 317422  
 317421  
 317420  
 317419  
 317418  
 317417  
 317416  
 317415  
 317414  
 317413  
 317412  
 317411  
 317410  
 317409  
 317408  
 317407  
 317406  
 317405  
 317404  
 317403  
 317402  
 317401  
 317400  
 317399  
 317398  
 317397  
 317396  
 317395  
 317394  
 317393  
 317392  
 317391  
 317390  
 317389  
 317388  
 317387  
 317386  
 317385  
 317384  
 317383  
 317382  
 317381  
 317380  
 317379  
 317378  
 317377  
 317376  
 317375  
 317374  
 317373  
 317372  
 317371  
 317370  
 317369  
 317368  
 317367  
 317366  
 317365  
 317364  
 317363  
 317362  
 317361  
 317360  
 317359  
 317358  
 317357  
 317356  
 317355  
 317354  
 317353  
 317352  
 317351  
 317350  
 317349  
 317348  
 317347  
 317346  
 317345  
 317344  
 317343  
 317342  
 317341  
 317340  
 317339  
 317338  
 317337  
 317336  
 317335  
 317334  
 317333  
 317332  
 317331  
 317330  
 317329  
 317328  
 317327  
 317326  
 317325  
 317324  
 317323  
 317322  
 317321  
 317320  
 317319  
 317318  
 317317  
 317316  
 317315  
 317314  
 317313  
 317312  
 317311  
 317310  
 317309  
 317308  
 317307  
 317306  
 317305  
 317304  
 317303  
 317302  
 317301  
 317300  
 317299  
 317298  
 317297  
 317296  
 317295  
 317294  
 317293  
 317292  
 317291  
 317290  
 317289  
 317288  
 317287  
 317286  
 317285  
 317284  
 317283  
 317282  
 317281  
 317280  
 317279  
 317278  
 317277  
 317276  
 317275  
 317274  
 317273  
 317272  
 317271  
 317270  
 317269  
 317268  
 317267  
 317266  
 317265  
 317264  
 317263  
 317262  
 317261  
 317260  
 317259  
 317258  
 317257  
 317256  
 317255  
 317254  
 317253  
 317252  
 317251  
 317250  
 317249  
 317248  
 317247  
 317246  
 317245  
 317244  
 317243  
 317242  
 317241  
 317240  
 317239  
 317238  
 317237  
 317236  
 317235  
 317234  
 317233  
 317232  
 317231  
 317230  
 317229  
 317228  
 317227  
 317226  
 317225  
 317224  
 317223  
 317222  
 317221  
 317220  
 317219  
 317218  
 317217  
 317216  
 317215  
 317214  
 317213  
 317212  
 317211

#### REFERENCES

1. Weeks, Richard F., Optics News, September 1975.
2. Fisher, R. W., Helmick, R. D., Licis, G., "Supplemental Technical Analysis for Remote Viewing System Effort," MCAIR Report A3808, 31 December 1975.
3. Ory, H. A., "Statistical Detection Theory," Rand Corporation Memo RM-5992-PR, September 1969.
4. Kingslake, R., "Applied Optics and Optical Engineering," Volume III, Academic Press, New York, 1965.



AFAL/RWI  
WRIGHT-PATTERSON AFB, OH 45433

United States Air Force  
Official Business

(Back Cover)